

COPYRIGHT NOTICE



FedUni ResearchOnline

<http://researchonline.federation.edu.au>

This is the author's accepted version of the following publication:

Armaghani, D., Momeni, E., Abad, S., Khandelwal, M. (2015) Feasibility of ANFIS model for prediction of ground vibrations resulting from quarry blasting. *Environmental Earth Sciences*, 74(4), 2845-2860.

The version displayed here may differ from the final published version.

The final publication is available at:

<http://doi.org/10.1007/s12665-015-4305-y>

Copyright © 2015, Springer-Verlag Berlin Heidelberg

1
2
3
4 **Feasibility of ANFIS Model for Prediction of Ground Vibrations Resulting from**
5
6
7 **Quarry Blasting**
8
9

10 Danial Jahed Armaghani^a, Ehsan Momeni^b, Seyed Vahid Alavi Nezhad Khalil Abad^c, Manoj Khandelwal^{d*}
11
12

13 ^a Department of Geotechnics and Transportation, Faculty of Civil Engineering, Universiti
14 Teknologi Malaysia, 81310, UTM, Skudai, Johor, Malaysia. Email:
15 danialarmaghani@yahoo.com.
16
17

18
19
20 ^b Department of Geotechnics and Transportation, Faculty of Civil Engineering, Universiti
21 Teknologi Malaysia, 81310, UTM, Skudai, Johor, Malaysia. Email: mehsan23@live.utm.my.
22
23

24
25
26 ^c Department of Geotechnics and Transportation, Faculty of Civil Engineering, Universiti
27 Teknologi Malaysia (UTM), Skudai 81310, Johor, Malaysia. Email: vankaseyed2@live.utm.my.
28

29
30
31 ^{d*} Faculty of Science and Technology, Federation University Australia, PO Box 663, Ballarat,
32 Victoria 3353, Australia Phone: +61 3 5327 9821 Email:
33 m.khandelwal@federation.edu.au (**Corresponding Author**).
34
35
36

37
38
39 **Abstract**
40

41
42 One of the most significant environmental issues of blasting operations is ground vibration which
43 can cause damage to the surrounding residents and structures. Hence, it is a major concern to
44 predict and subsequently control the ground vibration due to blasting. This paper presents two
45 artificial intelligence (AI) techniques namely adaptive neuro-fuzzy inference system (ANFIS) and
46 artificial neural network (ANN) for the prediction of ground vibration in quarry blasting site. For
47 this purpose, blasting parameters as well as ground vibrations of 109 blasting operations were
48 measured in ISB granite quarry, Johor, Malaysia. Moreover, an empirical equation was also
49 proposed based on the measured data. Several AI-based models were trained and tested using the
50 measured data to determine the optimum models. Each model involved two inputs (maximum
51
52
53
54
55
56
57
58
59
60
61
62
63
64
65

1
2
3
4 charge per delay and distance from the blast-face) and one output (ground vibration). To control
5
6 capacity performances of the predictive models, the values of root mean squared error (RMSE),
7
8 value account for (VAF), and coefficient of determination (R^2) were computed for each model. It
9
10 was found that the ANFIS model can provide better performance capacity in predicting ground
11
12 vibration in comparison with other predictive techniques. The values of 0.973, 0.987 and 97.345
13
14 for R^2 , RMSE and VAF, respectively reveal that the ANFIS model is capable to predict ground
15
16 vibration with high degree of accuracy.
17
18

19
20 **Keywords:** Blasting, Ground vibration, ANFIS, ANN, Empirical equation.
21

22 23 **1. Introduction**

24
25
26 Blasting is a common technique for rock fragmentation in quarries, mining operations and some
27
28 civil engineering applications such as tunneling and leveling/road construction. In quarry works,
29
30 several rows of blast-holes (almost parallel to the free face of the bench) are drilled and blasted.
31
32 These operations cause several impacts such as ground vibration, air-overpressure, flyrock, and
33
34 back-break in the blasting environmental zone (Khandelwal and Singh 2009; Jahed Armaghani et
35
36 al. 2013; Hajihassani et al. 2014a; Raina et al. 2014; Ebrahimi et al. 2015). Among them, ground
37
38 vibration is recognized as an undesirable phenomenon which may lead damage to the surrounding
39
40 structures (Singh and Singh 2005; Ozer et al. 2008)
41
42

43
44
45 When an explosive is detonated in a blast-hole, chemical reaction of the explosives produces a
46
47 high pressure and temperature gas. This gas pressure crushes the rock adjacent to the blast-hole.
48
49 The detonation pressure decays or dissipates quickly. A wave motion is created in the ground by
50
51 the strain waves conveyed to the surrounding rocks (Duvall and Petkof 1959). Due to various
52
53 breakage mechanism, like radial cracking, crushing, and reflection breakage in the free face, the
54
55 strain energy carried out by these strain waves fragments the rock mass (Khandelwal et al. 2011).
56
57 The strain waves are propagated as the elastic wave when the stress wave intensity reduces to the
58
59
60
61
62
63
64
65

1
2
3
4 ground level. These waves are known as ground vibration. The ground vibration can be spread
5
6 from the blast-hole in all direction (Dowding 1985).

7
8
9 High ground vibration can cause damage to the surrounding structures, groundwater conduits, and
10
11 ecology of the nearby area (Khandelwal and Singh 2006; Monjezi et al. 2010). The ground
12
13 vibrations are measured in terms of peak particle velocity (PPV) and frequency. As reported in
14
15 several standards (New 1986; Indian Standard 1973), PPV is considered as a vibration index,
16
17 which is a significant indicator to control the structural damage criteria. Several parameters such
18
19 as blast design, distance from the blast-face, explosive charge weight per delay, and geological
20
21 conditions are the most effective factors on ground vibration induced by blasting (Wiss and
22
23 Linehan 1978; Khandelwal and Singh 2007; Iphar et al. 2008).

24
25
26
27
28 Various empirical predictors have been suggested for the prediction of PPV (*e.g.* Duvall and
29
30 Petkof 1959; Langefors and Kihlstrom 1963; Davies et al. 1964; Ambraseys and Hendron 1968;
31
32 Roy 1993). Normally, in these approaches, PPVs are obtained from two factors namely maximum
33
34 charge per delay and distance from the blast-face. As a result, in many cases, these methods are
35
36 not accurate enough, whereas prediction of the PPV values with high accuracy is important to
37
38 estimate the blasting safety area. In addition, these empirical equations need to be updated when
39
40 new blasting data is available. Aside from the empirical equations, the use of statistical methods
41
42 such as multiple regression analysis in predicting PPV has received attention mainly due to their
43
44 ease of use (Hudaverdi 2012). However, the implementation of the statistical prediction
45
46 techniques is not reliable if new available data are different from the original ones (Khandelwal
47
48 and Singh 2009; Monjezi et al. 2013).

49
50
51
52
53 Besides, utilizing artificial intelligence (AI) methods such as artificial neural network (ANN) in
54
55 the field of earth science is recently highlighted in literatures. This may be attributed to AI
56
57 capability in solving non-linear continuous functions (Dehghan et al. 2010). Isik and Ozden
58
59 (2013) used ANN for predicting soil compaction parameters namely maximum dry unit weight
60
61

1
2
3
4 (σ_{dmax}) and optimum water content (w_{opt}). Ceryan et al. (2013) conducted a research to predict the
5
6 uniaxial compressive strength of carbonate rocks using ANN. In another study, Verma and Singh
7
8 (2013) showed capability of the ANN technique in predicting water quality parameters including
9
10 biological oxygen demand (BOD) and chemical oxygen demand (COD). Moreover, Park et al.
11
12 (2013) and Bi et al. (2014) applied ANN to estimate landslide susceptibility index (LSI).
13
14 Dissolved organic carbon (DOC) in a river network was evaluated and predicted using ANN in
15
16 the study conducted by Fu et al. (2013). An ANN toolbox was created within GIS software by
17
18 Lee et al. (2014). They successfully showed capability of this toolbox for solving geotechnical
19
20 problems. A hybrid ANN-based predictive model was developed to estimate pile bearing
21
22 capacity in the study carried out by Momeni et al. (2014). Ocak and Seker (2013) utilized ANN
23
24 technique for solving problem of surface settlement caused by tunneling. A comparative study
25
26 was performed by Maiti and Tiwari (2014) to predict groundwater level using ANN and adaptive
27
28 neuro-fuzzy inference system (ANFIS) models. It was found that ANN can perform better than
29
30 ANFIS for prediction of groundwater level. Gordan et al. (2015) proposed a hybrid particle
31
32 swarm optimization (PSO)-ANN to predict seismic stability of the homogeneous slopes.
33
34 Furthermore, several researchers have been used AI techniques in the case of PPV prediction.
35
36 Khandelwal and Singh (2006) utilized four empirical predictors to estimate the PPV values for
37
38 150 blasting operations and obtained results were compared to the measured data. Subsequently,
39
40 an ANN model was proposed for the prediction of PPV using the same data. They found that
41
42 ANN results are more accurate compared to empirical predictors. Fisne et al. (2011) used fuzzy
43
44 inference system (FIS) and regression analysis to predict PPV using 33 datasets obtained from
45
46 Akdaglar quarry in Turkey. In their research, charge weight and distance from blast-face were
47
48 considered as model inputs. They concluded that the FIS technique can predict PPV values better
49
50 than the statistical technique. Monjezi et al. (2013) predicted PPV values using ANN model and
51
52 the obtained results were compared to the recorded data in Shur River Dam, Iran as well as
53
54 obtained results by empirical equations. Finally, they concluded that the ANN model has higher
55
56
57
58
59
60
61

1
2
3
4 performance capacity compared to the empirical equations. Table 1 shows some recent studies
5
6 with their performances in predicting PPV induced by blasting. In this study, ANN and ANFIS
7
8 models have been developed to predict PPV resulting from blasting in granite quarry.
9
10 Additionally, an empirical equation was suggested for prediction of PPV values according to
11
12 USBM method recommended by Duvall and Petkof (1959). Eventually, results of PPV values
13
14 using empirical equation, ANN and ANFIS models, were compared and discussed.
15
16
17
18
19

20 **2. Case Study and Data Monitoring**

21
22 The data used in this study was collected from ISB granite quarry, Kota Tinggi, Johor, Malaysia.
23
24 The quarry lies geographically in latitude $1^{\circ} 44' 12''$ N and longitude $103^{\circ} 54' 08''$ E, and is
25
26 located 40 km north of Johor Bahru (Fig. 1). This quarry supplies granite aggregates for many
27
28 construction applications with capacity of 37000-44000 ton per month. Depend on the weather
29
30 condition, 4 to 8 blasting works per month were performed in this site. All blasting operations
31
32 were performed using blast-hole diameters of 89 mm and 115 mm. ANFO and dynamite were
33
34 used as the main explosive material and initiation respectively. The blast-holes were stemmed
35
36 using fine gravels.
37
38

39
40 During data collection, blasting parameters including hole diameter, hole depth, maximum charge
41
42 per delay, burden, spacing, stemming length, powder factor and number of hole were measured.
43
44 In addition, in each blasting, PPV was monitored using Vibra ZEB seismograph having
45
46 transducers for PPV measurement. The nearest structure is located about 450 m to the south of
47
48 the quarry. It should be mentioned that the distances between monitoring point and blast-face
49
50 were set in the range of 125 m to 670 m. Hole depths used in the blasting operations were in the
51
52 range of 13.5 m and 26.5 m. In total, 109 blast were recorded and PPV in each blasting operation
53
54 was monitored. In this study, among all measured blasting parameters, only maximum charge per
55
56 delay (MC) and distance between monitoring point and blast-face (D) were taken into
57
58
59
60
61

1
2
3
4 consideration for the prediction of PPV values as recommended by Duvall and Petkof (1959). In
5
6 addition, the mentioned parameters have been extensively-used as predictor in many PPV
7
8 prediction studies (see Table 1). Figs. 2-4 show the frequency of measured values of maximum
9
10 charge per delay, distance between monitoring point and blast-face and PPV, respectively.
11
12
13

14 **3. Empirical Equation Development**

15
16 Numerous PPV equations have been established empirically by many researchers (e.g.
17
18 Ambraseys and Hendron 1968; Roy 1993). The most popular PPV equation is a typical method
19
20 suggested by Duvall and Petkof (1959). In the absence of monitoring, the use of scaled distance
21
22 (SD) factor is a method for prediction of PPV. A relationship between the MC and D values is
23
24 formed through the SD formula as follows:
25
26
27
28

$$\sqrt{\frac{W}{D}} \quad (1)$$

30
31 Where W is the maximum charge per delay (kg) and D represents the distance between
32
33 monitoring point and blast-face (m). Afterward, PPV values can be determined using the
34
35 suggested equation by Duvall and Petkof (1959) as follows:
36
37
38
39

$$(2)$$

40
41 In which B and K are site constants. By using measured data from ISB granite quarry and also
42
43 necessary analysis by SPSS (18.0), an empirical formula was suggested to predict PPV values as:
44
45
46

$$(3)$$

47
48 Coefficient of determination, R^2 , equals to 0.836 for the Eq. 3 indicates that the proposed
49
50 empirical equation can predict PPV with suitable accuracy level. Logarithmic graph between
51
52 monitored PPVs and scaled distance values is shown in Fig. 5.
53
54
55
56

57 **4. Artificial Intelligence Techniques for PPV Prediction**

58 **4.1 Artificial Neural Network (ANN)**

1
2
3
4 ANNs are information processing patterns simulating the biological nervous systems which
5
6 figure out the existing function from actual data. In other words, an ANN is a flexible non-linear
7
8 function approximation that estimates a relationship between given input and output parameters.
9
10 ANNs learn by examples in order to obtain a connection through the parameters. The earliest
11
12 neuron was introduced by McCulloch and Pitts (1943), called the “Threshold Logic Unit”. Their
13
14 model describes a neuron as a linear threshold, equivalent to using the unit step function; the
15
16 function value is 0, if the nerve cell remains inactive, or 1, if the cell fires. Nevertheless, the first
17
18 ANN was developed by Rosenblatt (1958), called the “perceptron” based on the neuron of
19
20 McCulloch and Pitts (1943).
21
22

23
24 ANNs are composed of a set of parallel interconnected processing units titled nodes or neurons.
25
26 There is an activation function along each neuron which transfers the activation signal between
27
28 nodes. However, the ability of an ANN in data processing is mainly related to its architecture and
29
30 weights (Dreyfus 2005; Engelbrecht 2007). In terms of the structure, ANNs are divided into two
31
32 types; feed-forward and recurrent ANNs. In feed-forward ANNs, the neurons are usually
33
34 classified into several layers. Using the connections, a signal moves throughout the input to the
35
36 output layer(s). Multi-layer perceptron (MLP) is the most well-known type of feed-forward
37
38 ANNs (Kosko 1994). In recurrent ANNs, the outputs of some (or all) neurons are fed back to the
39
40 same neuron or into neurons in preceding layers. Therefore, the signals can move both forward
41
42 and backward. Compared to other types of ANNs, feed forward MLP ANN is not complicated to
43
44 implement (Bounds et al. 1998). This type of ANN has been applied successfully in various areas
45
46 of engineering problems (Meulenkamp and Grima 1999; Singh et al. 2001; Tonnizam Mohamad
47
48 et al. 2014).
49
50
51

52
53 The ability of ANNs to learn from samples and improve their performance is obtained by learning
54
55 algorithm. Back-propagation (BP) algorithm is the most common training algorithm that tries to
56
57 adjust the network weights during learning process by reducing the error between input and
58
59
60
61

1
2
3
4 output data (Specht 1991). Fundamentally, BP learning consists of forward and backward passes
5
6 in various layers of the network. The input parameters are applied to the hidden neurons and
7
8 subsequently the outputs are produced. The error correction is conducted if the outputs of the
9
10 network are different from the desired values. This action is conducted through the adjustment of
11
12 weights and biases in which BP algorithm utilized for this purpose (Basheer and Hajmeer 2000).
13
14 Eventually, the system error can be computed based on some performance criteria such as root
15
16 mean square error (RMSE) (Kosko 1994; Simpson 1990).
17
18

19 20 **4.2 PPV Prediction by ANN**

21
22 As mentioned previously, maximum charge per delay and distance between monitoring point and
23
24 blast-face were considered as model inputs for prediction of PPV values. More detail of the input
25
26 and output parameters are shown in Table 2. In this study, all datasets were normalized by using
27
28 following equation:
29

$$30 \quad X_{norm} = (X - X_{min}) / (X_{max} - X_{min}) \quad (4)$$

31
32 Where X is the measured value, X_{norm} is the normalized value of the measured parameter; X_{min}
33
34 and X_{max} are the minimum and maximum values of the measured parameters in the dataset,
35
36 respectively. Afterwards, all 109 datasets were divided into training and testing datasets. In this
37
38 regard, 80% of the datasets were assigned for training purposes while the other 20% was used for
39
40 testing of the network performance. To achieve the premier ANN performance, optimal network
41
42 architecture should be determined. Hornik et al. (1989) stated that only one hidden layer in the
43
44 network architecture can estimate any continuous function. Hence, in this study, one hidden layer
45
46 was used. Aside from the number of hidden layer, in ANN architecture, selecting the number of
47
48 nodes in the hidden layer is the most critical task (Sonmez et al. 2006). Many relations have been
49
50 established to determine the number of nodes in hidden layers by some scholars as it can be seen
51
52 in Table 3. According to this table, using two inputs and one output, the number of nodes which
53
54 should be used in the hidden layer varies between one and six. In the next step of the analysis, the
55
56
57
58
59
60
61

1
2
3
4 optimum number of nodes in the hidden layer must be determined. For this purpose, several
5
6 networks with one hidden layer were trained and tested to predict PPV values as shown in Table
7
8
9 4. As tabulated in this table, each model was repeated five times by using the random
10 distributions of datasets. In this table, results in terms of RMSE are listed for training and testing
11 datasets, whereas RMSE values for testing datasets were set as performance criteria. Model
12
13 number 6 with six hidden nodes (second iteration) indicates higher prediction performance
14
15 compared to other models in predicting PPV. Therefore, this model with two inputs, one hidden
16
17 layer and six nodes in the hidden layer was selected as the best ANN model. It is also worth
18
19 mentioning that in construction of ANN models, the learning rate and momentum coefficient
20
21 were set to be 0.1 and 0.9 respectively.
22
23
24

25 26 27 **4.3 Adaptive Neuro-Fuzzy Inference System**

28
29 The adaptive neuro-fuzzy inference system (ANFIS) was first introduced by Jang (1993). Study
30
31 by Jung et al. (1997) recommends ANFIS capability in approximating any actual continuous
32
33 function. ANFIS is capable of simulating a functional mapping which approximates the
34
35 prediction process of the internal system parameter. The term neuro-fuzzy is used due to the fact
36
37 that in this artificial intelligence methods, the FIS concept is integrated into the ANN. Many
38
39 researchers have addressed the successful application of ANFIS in solving geotechnical problems
40
41 (Grima et al. 2000; Singh et al. 2012; Yesiloglu-Gultekin et al. 2013; Jahed Armaghani et al.
42
43 2014). In fact, the prime objective of ANFIS is to map a relationship between the input and
44
45 output parameters. This can be done through a hybrid learning procedure for determination of the
46
47 membership function (MF) distribution. A classic ANFIS network architecture comprising two
48
49 input parameters x , y and a single output parameter f is presented in Fig. 6. As shown in this
50
51 figure, the architecture consists of multiple layers *i.e.* 5 in the inference system, and each layer
52
53 includes a number of neurons, which are defined by the neuron function.
54
55
56
57
58
59
60
61
62
63
64
65

In the previous layers, the output node is recognized as the feeding data of the present layer. After applying an operation using neuron function in the present layer, the model output forms the input signals of the next layer. To briefly illustrate the ANFIS procedure, consider a FIS model comprising, x and y as inputs and f as output. Hence, two fuzzy ‘‘if-then’’ rules can be introduced as shown in the following lines:

(rule 1)

(rule 2)

where, A_1, A_2, B_1, B_2 are defined as MFs for inputs x and y ; $p_1, q_1, r_1, p_2, q_2, r_2$ are the output function parameters. In the following, the five-layer ANFIS comprising two fuzzy rules, x and y (inputs) and one output (f) is discussed (Jang 1993):

Layer 1: All neurons i in this layer are adaptive neurons.

$$O_{1,i} = \mu A_i(x) \tag{5}$$

$$O_{1,i} = \mu B_i(y) \tag{6}$$

For $i=1, 2$ where x and y are set as input nodes, and A and B are the linguistic labels. Also, $\mu A_i(x)$ and $\mu B_i(y)$ symbolize the MFs.

Layer 2: The neurons are labeled Π and shown by a circle. The output node, then, is formed based on incoming signals.

$$O_{2,i} = \omega_i = \mu A_i(x) \mu B_i(y) \text{ with } i = 1,2 \tag{7}$$

The output node ω_i indicates the firing strength of a rule.

Layer 3: Every neuron in this layer is a fixed neuron to be identified by a circle and labeled as N .

The output is obtained based on the ratio of the i^{th} rule’s firing strength over the summation of firing strength of all rules.

$$O_{3,i} = \varpi_i = \omega_i / (\omega_1 + \omega_2) \text{ with } i = 1,2 \quad (8)$$

Layer 4: In this layer, every neuron is an adaptive neuron with the neuron function like this:

$$O_{4,i} = \varpi_i f_i = \varpi_i (p_i x + q_i y + r_i) \quad (9)$$

Where parameters p_i, q_i, r_i are typically known as consequent parameters and ϖ_i denotes normalized firing strength.

Layer 5: In this layer the final step is taken. This step deals with generating the output amount through summation of all incoming signals:

$$O_{5,i} = \sum_i \varpi_i f_i = \sum_i \varpi_i f_i / \sum_i \varpi_i; \quad i = 1,2 \quad (10)$$

Back-propagation gradient descent forms the basic training rule of ANFIS. In this learning algorithm, the error signals from the output layer backward to the input neuron are recursively determined. Based on the architecture presented in Fig. 6 (b), the output (f) can be presented as a linear group of the consequent parameters. To learn the fuzzy model employing differentiable functions, ANFIS employ a hybrid-learning rule due to its ease of use. The conventional BP algorithm is mainly utilized by ANFIS to train the MF parameters. Also, the classic least-squares predictor is applied by ANFIS to train the parameter of the first-order polynomial of the Takagi–Sugeno–Kang fuzzy model as stated in a study by Jang et al. (1997).

The hybrid training algorithm of ANFIS uses so-called forward and backward passes. In the former, functional signals go forward till layer 4 and the consequent parameters are estimated using least-squares error criteria. Subsequently, like ANN procedure, to update the premise parameters, the obtained errors are backwardly propagated. This process is repeated using gradient descent method until reaching a desirable output. The final output can be illustrated in the following manner:

1
2
3
4
5
6
7
8
9
10
11
12
13
14
15
16
17
18
19
20
21
22
23
24
25
26
27
28
29
30
31
32
33
34
35
36
37
38
39
40
41
42
43
44
45
46
47
48
49
50
51
52
53
54
55
56
57
58
59
60
61
62
63
64
65

$$\frac{\mu_{A_1}(x) \mu_{B_1}(y)}{\mu_{A_1}(x) \mu_{B_1}(y) + \mu_{A_2}(x) \mu_{B_2}(y)} \mu_{A_2}(x) \mu_{B_2}(y) + \frac{\mu_{A_1}(x) \mu_{B_2}(y) \mu_{A_2}(x) \mu_{B_1}(y)}{\mu_{A_1}(x) \mu_{B_2}(y) + \mu_{A_2}(x) \mu_{B_1}(y)} \mu_{A_1}(x) \mu_{B_1}(y) \quad (11)$$

where $p_1, q_1, r_1, p_2, q_2,$ and r_2 are consequent parameters. The prime advantage of implementing an ANFIS model is efficient determination of the consequent and optimal premise parameters during training procedure.

4.4 PPV Prediction by ANFIS

This paper provides an insight into the application of ANFIS for predicting PPV. Similar to ANN part, the required datasets for modelling were randomly divided into two subsets: 80% of the dataset was set for training the model and the rest was considered for testing purposes. In this study, the numbers of fuzzy rules were determined using a trial-error method. Numerous models with different fuzzy rule combinations (e.g. 2, 3 and so on) were used for this reason. Eventually, it was concluded that the ANFIS structure with 5MFs for each input performs best when the results of RMSE were compared. In overall, the conducted parametric study suggested that the best prediction performance of the model is expected when ANFIS model is trained with 25 fuzzy roles (5 5). The type of MF utilized for each input is the Gaussian MF. Gaussian MFs are the most well-known MF in the literatures of fuzzy system, as they provide both simplicity and flexibility (Tutmez et al. 2007). In the next step of the modeling, ANFIS models were built to predict PPV values. Prediction performances of these models are shown in Table 5. This table indicates that PPV values were repeated 5 times using different training and testing datasets randomly. According to the presented results in this table, model number 4 outperforms other models. Hence, the aforementioned model *i.e.* model number 4 was chosen for prediction of PPV. RMSE values equal to 0.983 and 1.017 for training and testing datasets show the high performance capacity of the ANFIS model in predicting PPV. In model number 4, the MFs of the inputs were adjusted after 29,700 epochs using the hybrid optimization method. This optimization

1
2
3
4 method includes BP for the parameters associated with the input MFs and also estimation of
5
6 least-squares for the parameters associated with the output MFs.

7
8
9 Figs.7 and 8 display the assigned input MFs after training step. The linguistic variables assigned
10
11 for “maximum charge weight per delay” and “distance” are very low (VL), low (L), medium
12
13 (M), high (H), very high (VH), and very close (VC), close (C), normal (N), far (F), very far (VF),
14
15 respectively. Additionally, the type of output membership function was set to be linear. It should
16
17 be mentioned that all ANN and ANFIS predictive models were constructed using MATLAB
18
19 (version 7.14.0.739). SPSS package (18.0) was used to determine RMSE values as well as
20
21 statistical calculations. The suggested ANFIS structure is shown in Fig. 9.
22
23

24 25 **5. Results and Discussion**

26
27
28 In this study, an attempt has been made to examine the ability of ANN and ANFIS models for
29
30 prediction of PPV values induced by quarry blasting. For this purpose, a database comprising of
31
32 109 blasting operations was prepared. Several ANN and ANFIS models were built using two
33
34 inputs namely maximum charge per delay and the distance from the blast-face. Additionally,
35
36 using the same datasets based on suggested method by Duvall and Petkof (1959), an empirical
37
38 equation was proposed. Fig. 10 shows the PPV values predicted by empirical equation against
39
40 monitored PPVs. R^2 value equal to 0.836 reveals that this equation is able to predict PPV with
41
42 suitable accuracy. Fig. 11 displays the predicted PPVs by employing conventional ANN
43
44 technique plotted against the measured PPV values for training and testing datasets. The R^2
45
46 values of 0.955 and 0.902 for training and testing datasets show that the ANN approach can
47
48 predict PPV with high accuracy level. Moreover, in the prediction of PPV using the ANFIS
49
50 technique, R^2 values of 0.974 and 0.969 for training and testing datasets suggest the superiority of
51
52 this technique in predicting PPV compared to proposed empirical equation and ANN technique
53
54 (see Fig. 12).
55
56
57
58
59
60
61

In order to demonstrate the capability of developed models, the widely-used PPV empirical equations were applied. Table 6 shows these PPV predictor equations as well as their site constants for granite. Using the presented equations in Table 6 and collected parameters from the site, PPV values were predicted. Figs 13 to 17 illustrate measured PPVs against predicted PPVs by Langefors – Kihlstrom, general predictor, Indian standard, Ghosh - Daemen predictor, and CMRI equations, respectively. The results show lower performance capacities of the empirical models in comparison to proposed models in this study.

To check the capacity performance of the predictive models as well as empirical PPV predictors, vales of RMSE and value account for (VAF) were obtained as follows:

$$RMSE = \sqrt{\frac{\sum (y - y')^2}{N}}, \quad (12)$$

$$VAF = [1 - \frac{\sum (y - y')^2}{\sum (y - \bar{y})^2}], \quad (13)$$

Where y and y' are the obtained and predicted values, respectively and N is the total number of data. When the RMSE value is zero and VAF value is 100, the model's performance is perfect. Table 7 shows the performance indices achieved by all mentioned models in this study. As it can be seen in this table, the ANFIS model can provide higher performance capacity in predicting PPV induced by blasting compared to other predictive techniques. The values of 0.973, 0.987 and 97.345 for R^2 , RMSE and VAF respectively reveal that the ANFIS model is capable to predict PPV with high degree of accuracy. It is important to note that proposed model based on USBM in this study can predict PPV values better than empirical PPV predictors. This can be seen clearly based on obtained RMSE values. RMSE value of 2.469 for proposed model based on USBM shows superiority of this model in predicting PPV, while these values were obtained as 10.473, 6.391, 7.821, 6.233 and 4.078 for Langefors – Kihlstrom, general predictor, Indian standard, Ghosh - Daemen predictor, and CMRI models, respectively. The presented results show that all

1
2
3
4 proposed models are able to estimate PPV induced by quarry blasting. Nevertheless, the ANFIS
5
6 model may be used when PPV values with higher degree of accuracy is required. Cautious step
7
8 needs to be taken when the range of future data is beyond the range of the data used in this study.
9

10 11 12 **6. Conclusions**

13
14 In this study, several models have been proposed to predict ground vibration induced by quarry
15
16 blasting. The model dataset include blasting parameters and PPV values of 109 blasting works in
17
18 ISB granite quarry, Johor, Malaysia. The maximum charge per delay and distance from blast-face
19
20 were considered as model inputs for prediction of PPVs. Several ANN and ANFIS models were
21
22 trained and tested using the mentioned inputs-output configuration and finally two models were
23
24 chosen as best models of ANN and ANFIS. Apart from that, using the same input parameters, a
25
26 model based on USBM was proposed for prediction of PPV values. To show the ability of the
27
28 proposed models, some empirical predictors were also applied to predict PPVs. Finally, the
29
30 results indicated that the ANFIS predictive model is able to predict PPVs with higher accuracy
31
32 compared to other models. It is worth noting that in practice all proposed methods have the
33
34 applicability of PPV prediction. However, depending on the condition, they should be used
35
36 accordingly.
37
38
39

40 41 42 **Acknowledgement**

43
44 The authors would like to extend their appreciation to the Universiti Teknologi Malaysia for all
45
46 facilities that made this research possible.
47

48 49 **References**

- 50
51
52 Ambraseys NR, Hendron AJ (1968) Dynamic Behavior of Rock Masses: Rock Mechanics in Engineering
53
54 Practices. London: Wiley
55
56
57 Basheer IA, Hajmeer M (2000) Artificial neural networks: fundamentals, computing, design, and
58
59 application. J Microbiol Meth 43:3-31
60
61

- 1
2
3
4 Bi R, Schleier M, Rohn J, Ehret D, Xiang W (2014) Landslide susceptibility analysis based on ArcGIS and
5
6 Artificial Neural Network for a large catchment in Three Gorges region, China. Environ Earth Sci
7
8 72(6):1925-1938
9
- 10
11 Bounds DG, Lloyd PJ, Mathew B, Waddell G (1998) A multilayer perceptron network for the diagnosis of
12
13 low back pain In Neural Networks. IEEE International Conference 481-489
14
15
- 16
17 Bureau of Indian Standard (1973) Criteria for safety and design of structures subjected to underground
18
19 blast. ISI Bull IS-6922
20
- 21
22 Ceryan N, Okkan U, Kesimal A (2013) Prediction of unconfined compressive strength of carbonate rocks
23
24 using artificial neural networks. Environ Earth Sci 68(3):807-819
25
- 26
27 Davies B, Farmer IW, Attewell PB (1964) Ground vibrations from shallow sub-surface blasts. The
28
29 Engineer 217: 553–559
30
- 31
32 Dehghan S, Sattari GH, Chehreh CS, Aliabadi MA (2010) Prediction of unconfined compressive strength
33
34 and modulus of elasticity for Travertine samples using regression and artificial neural. New Min
35
36 Sci Technol 20:0041-0046
37
- 38
39 Dowding CH (1985) Blast vibration monitoring and control. Englewoods Cliffs, NJ: Prentice-Hall pp, 288-
40
41 290
42
- 43
44 Dreyfus G (2005) Neural Networks: methodology and application. (2nd ed.), Springer, Berlin Heidelberg,
45
46 Germany
47
- 48
49 Duvall WI, Petkof B (1959) Spherical Propagation of Explosion Generated Strain Pulses in Rock. USBM
50
51 Report of Investigation 5483, 21
52
- 53
54 Ebrahimi E, Monjezi M, Khalesi MR, Jahed Armaghani D (2015) Prediction and optimization of back-
55
56 break and rock fragmentation using an artificial neural network and a bee colony algorithm. Bull
57
58 Eng Geol Environ DOI 10.1007/s10064-015-0720-2
59
- 60
61 Engelbrecht AP (2007) Computational intelligence: an introduction. John Wiley & Sons
62
63
64
65

- 1
2
3
4 Fisne A, Kuzu C, Hüdaverdi T (2011) Prediction of environmental impacts of quarry blasting operation
5
6 using fuzzy logic. *Environ Monit Assess* 174:461-470
7
8
- 9 Fu Y, Zhao Y, Zhang Y, Guo T, He Z, Chen J (2013) GIS and ANN-based spatial prediction of DOC in
10
11 river networks: a case study in Dongjiang, Southern China. *Environ Earth Sci* 68(5):1495-1505
12
13
- 14 Ghasemi E, Ataei M, Hashemolhosseini H (2013) Development of a fuzzy model for predicting ground
15
16 vibration caused by rock blasting in surface mining. *J Vib Control* 19(5):755-770
17
18
- 19 Ghoraba S, Monjezi M, Talebi N, Moghadam MR, Jahed Armaghani D (2015) Prediction of ground
20
21 vibration caused by blasting operations through a neural network approach: a case study of Gol-E-
22
23 Gohar Iron Mine, Iran. *J Zhejiang University Sci A* doi:10.1631/jzus.A1400252
24
- 25 Gordan B, Jahed Armaghani D, Hajihassani M, Monjezi M (2015) Prediction of seismic slope stability
26
27 through combination of particle swarm optimization and neural network. *Eng Comput*
28
29 doi:10.1007/s00366-015-0400-7
30
31
- 32 Grima MA, Bruines PA, Verhoef PNW (2000) Modeling tunnel boring machine performance by neuro-
33
34 fuzzy methods. *Tunn Undergr Sp Technol* 15(3):260–269
35
36
- 37 Hajihassani M, Jahed Armaghani D, Sohaei H, Tonnizam Mohamad E, Marto A (2014a) Prediction of
38
39 airblast-overpressure induced by blasting using a hybrid artificial neural network and particle
40
41 swarm optimization. *Appl Acoust* 80:57–67
42
43
- 44 Hajihassani M, Jahed Armaghani D, Marto A, Tonnizam Mohamad E (2014b) Ground vibration prediction
45
46 in quarry blasting through an artificial neural network optimized by imperialist competitive
47
48 algorithm. *Bull Eng Geol Environ* doi: 10.1007/s10064-014-0657-x
49
50
- 51 Hecht-Nielsen R (1987) Kolmogorov's mapping neural network existence theorem. *Proceedings of the first*
52
53 *IEEE international conference on neural networks*, San Diego CA, USA, pp 11-4
54
55
- 56 Hornik K, Stinchcombe M, White H (1989) Multilayer feedforward networks are universal Approximators.
57
58 *Neural Networks* 2:359-366
59
60
61
62
63
64
65

- 1
2
3
4 Hudaverdi T (2012) Application of multivariate analysis for prediction of blast-induced ground vibrations.
5
6 Soil Dyn Earthq Eng 43:300-308
7
8
9 Hush DR (1989) Classification with neural networks: a performance analysis. Proceedings of the IEEE
10 international conference on systems Engineering Dayton Ohia, USA, pp 277-80
11
12
13
14 Iphar M, Yavuz M, Ak H (2008) Prediction of ground vibrations resulting from the blasting operations in
15 an open-pit mine by adaptive neuro-fuzzy inference system. Environ Geol 56(1):97-107
16
17
18 Isik F, Ozden G (2013) Estimating compaction parameters of fine-and coarse-grained soils by means of
19 artificial neural networks. Environ Earth Sci 69(7):2287-2297
20
21
22
23 Jahed Armaghani D, Tonnizam Mohamad E, Momeni E, Narayanasamy MS, Mohd Amin MF (2014) An
24 adaptive neuro-fuzzy inference system for predicting unconfined compressive strength and
25 Young's modulus: a study on Main Range granite. Bull Eng Geol Environ doi:10.1007/s10064-
26
27 014-0687-4
28
29
30
31
32 Jahed Armaghani D, Hajihassani M, Mohamad ET, Marto A, Noorani SA (2013) Blasting-induced flyrock
33 and ground vibration prediction through an expert artificial neural network based on particle
34 swarm optimization. Arab J Geosci doi:10.1007/s12517-013-1174-0
35
36
37
38
39 Jang RJS (1993) Anfis: adaptive-network-based fuzzy inference system. IEEE Trans Syst Man Cybern
40 23:665–685
41
42
43
44 Jang RJS, Sun CT, Mizutani E (1997) Neuro-fuzzy and soft computing. Prentice-Hall, Upper
45 Saddle River, p 614
46
47
48 Kaastra I, Boyd M (1996) Designing a neural network for forecasting financial and economic time series.
49 Neurocomputing 10:215-36
50
51
52
53 Kanellopoulos I, Wilkinson GG (1997) Strategies and best practice for neural network image classification.
54 Int J Remote Sensing 18:711-25
55
56
57
58 Khandelwal M, Singh TN (2009) Prediction of blast-induced ground vibration using artificial neural
59 network. Int J Rock Mech Min Sci 46:1214-1222
60
61

- 1
2
3
4 Khandelwal M, Kumar DL, Yellishetty M (2011) Application of soft computing to predict blast-induced
5
6 ground vibration. *Eng Comput* 27(2):117-125
7
8
9 Khandelwal M, Singh TN (2006) Prediction of blast induced ground vibrations and frequency in opencast
10
11 mine-a neural network approach. *J Sound Vib* 289:711-725
12
13
14 Khandelwal M, Singh TN (2007) Evaluation of blast-induced ground vibration predictors. *Soil Dyn Earthq*
15
16 *Eng* 27(2):116-125
17
18 Kosko B (1994) *Neural networks and fuzzy systems: a dynamical systems approach to machine*
19
20 *intelligence*. Prentice Hall: New Delhi
21
22
23 Langefors U and Kihlstrom B (1963) *The modern technique of rock blasting*. New York: Wiley
24
25
26 Lee S, An H, Yu S, Oh JJ (2014) Creating an advanced backpropagation neural network toolbox within
27
28 GIS software. *Environ Earth Sci* 72(8):3111-3128
29
30
31 Li DT, Yan JL, Zhang L (2012) Prediction of Blast-Induced Ground Vibration Using Support Vector
32
33 Machine by Tunnel Excavation. *Appl Mech Mater* 170:1414-1418
34
35
36 Masters T (1994) *Practical neural network recipes in C++*. Boston MA: Academic Press
37
38
39 Maiti S, Tiwari RK (2014) A comparative study of artificial neural networks, Bayesian neural networks and
40
41 adaptive neuro-fuzzy inference system in groundwater level prediction. *Environ Earth*
42
43 *Sci* 71(7):3147-3160
44
45
46 McCulloch WS, Pitts W (1943) A logical calculus of the ideas immanent in nervous activity. *Bull Math*
47
48 *Biophys J* 5:115-133
49
50
51 Meulenkamp F, Grima MA (1999) Application of neural networks for the prediction of the unconfined
52
53 compressive strength (UCS) from Equotip hardness. *Int J Rock Mech Min Sci* 36(1):29-39
54
55
56 Mohamed MT (2011) Performance of fuzzy logic and artificial neural network in prediction of ground and
57
58 air vibrations. *Int J Rock Mech Min Sci* 48(5):845-851
59
60
61
62
63
64
65

- 1
2
3
4 Mohamadnejad M, Gholami R, Ataei M (2012) Comparison of intelligence science techniques and
5
6 empirical methods for prediction of blasting vibrations. *Tunn Undergr Sp Technol* 28:238-244
7
8
9 Momeni E, Nazir R, Jahed Armaghani D, Maizir H (2014) Prediction of Pile Bearing Capacity Using a
10
11 Hybrid Genetic Algorithm-Based Ann. *Measurement* 57:122–131
12
13
14 Monjezi M, Ahmadi M, Sheikhan A, Bahrami M, Salimi AR (2010) Predicting blast-induced ground
15
16 vibration using various types of neural networks. *Soil Dyn Earthq Eng* 30:1233-1236
17
18
19 Monjezi M, Hasanipanah M, Khandelwal M (2013) Evaluation and prediction of blast-induced ground
20
21 vibration at Shur River Dam, Iran, by artificial neural network. *Neural Comput Appl* 22:1637-
22
23 1643
24
25
26 Monjezi M, Ghafurikalajahi M, Bahrami A (2011) Prediction of blast-induced ground vibration using
27
28 artificial neural networks. *Tunn Undergr Sp Technol* 26(1):46-50
29
30
31 New BM (1986) Ground vibration caused by civil engineering works. *Transport and Road Research*
32
33 *Laboratory Research Report*, 53, 19
34
35
36 Ocak I, Seker SE (2013) Calculation of surface settlements caused by EPBM tunneling using artificial
37
38 neural network, SVM, and Gaussian processes. *Environ Earth Sci* 70(3):1263-1276
39
40
41 Ozer U, Kahriman A, Aksoy M, Adiguzel D, Karadogan A (2008) The analysis of ground vibrations
42
43 induced by bench blasting at Akyol quarry and practical blasting charts. *Environ Geol* 54:737-43
44
45
46 Paola JD (1994) Neural network classification of multispectral imagery. MSc thesis, The University of
47
48 Arizona, USA
49
50
51 Park S, Choi C, Kim B, Kim J (2013) Landslide susceptibility mapping using frequency ratio, analytic
52
53 hierarchy process, logistic regression, and artificial neural network methods at the Inje area,
54
55 Korea. *Environ Earth Sci* 68(5):1443-1464
56
57
58 Raina AK, Murthy VMSR, Soni AK (2014) Flyrock in bench blasting: a comprehensive review. *Bull. Eng.*
59
60
61 *Geol Environ* doi:10.1007/s10064-014-0588-6
62
63
64
65

- 1
2
3
4 Ripley BD (1993) Statistical aspects of neural networks. In: Barndoff- Neilsen OE, Jensen JL, Kendall WS,
5
6 editors. Networks and chaos-statistical and probabilistic aspects. London: Chapman & Hall, pp 40-
7
8 123
9
- 10 Roy PP (1993) Putting ground vibration predictors into practice. J Colliery Guardian 241:63-67
11
12
13
- 14 Rosenblatt F (1958) The perceptron: a probabilistic model for information storage and organization in the
15
16 brain. Psychological Review 65:386
17
18
- 19 Simpson PK (1990) Artificial neural system: foundation, paradigms applications and implementations.
20
21 New York, Pergamon
22
- 23 Singh TN and Singh V (2005) An intelligent approach to prediction and control ground vibration in mines.
24
25 Geotech Geolog Eng 23:249-262
26
- 27 Specht DF (1991) A general regression neural network Neural Networks. IEEE Transactions 2:568-576
28
29
30
- 31 Sonmez H, Gokceoglu C, Nefeslioglu HA, Kayabasi A (2006) Estimation of rock modulus: for intact rocks
32
33 with an artificial neural network and for rock masses with a new empirical equation. Int J Rock
34
35 Mech Min Sci, 43:224-235
36
37
- 38 Singh R, Kainthola A, Singh TN (2012) Estimation of elastic constant of rocks using an ANFIS
39
40 approach. Appl Soft Comput 12(1):40-45
41
42
- 43 Singh VK, Singh D, Singh TN (2001) Prediction of strength properties of some schistose rocks from
44
45 petrographic properties using artificial neural networks. Int J Rock Mech Min Sci 38(2):269-284
46
47
- 48 Tonnizam Mohamad E, JahedArmaghani D, Momeni E, AlaviNezhad Khalil Abad SV (2014) Prediction of
49
50 the unconfined compressive strength of soft rocks: a PSO-based ANN approach. Bull EngGeol
51
52 Environ doi:10.1007/s10064-014-0638-0
53
- 54 Tutmez B, Dag A, Tercan AE, Kaymak U (2007) Lignite thickness estimation via adaptive fuzzy-neural
55
56 network. In: 20th internationalmining congress and exhibition of Turkey-IMCET2007,Ankara, 6-
57
58 8 June 2007
59
60
61

1
2
3
4
5
6
7
8
9
10
11
12
13
14
15
16
17
18
19
20
21
22
23
24
25
26
27
28
29
30
31
32
33
34
35
36
37
38
39
40
41
42
43
44
45
46
47
48
49
50
51
52
53
54
55
56
57
58
59
60
61
62
63
64
65

Verma AK, Singh TN (2013) Prediction of water quality from simple field parameters. Environ Earth Sci
69(3):821-829

Wang C (1994) A theory of generalization in learning machines with neural application. PhD thesis, The
University of Pennsylvania, USA

Wiss JF, Linehan PW (1978) Control of vibration and air noise from surface coal Mines-III. US Bureau of
Mines Report OFR 103(3)-79, p 623

Yesiloglu-Gultekin N, Gokceoglu C, Sezer EA (2013) Prediction of uniaxial compressive strength of
granitic rocks by various nonlinear tools and comparison of their performances. Int J Rock Mech
Min Sci 62:113-122

1
2
3
4 **List of Figures:**
5

6
7 **Fig. 1** Map view of Kota Tinggi
8

9
10 **Fig. 2** Frequency histogram of measured MC values
11

12
13 **Fig. 3** Frequency histogram of measured D values
14

15
16 **Fig. 4** Frequency histogram of monitored PPV values
17

18
19 **Fig. 5** PPV values against scaled distance
20

21
22 **Fig. 6** (a) Sugeno fuzzy model with two rules, (b) equivalent ANFIS architecture [54]
23

24
25 **Fig. 7** Assigned MF for maximum charge per delay
26

27
28 **Fig. 8** Assigned MF for distance between monitoring point and blast-face
29

30
31 **Fig. 9** Suggested ANFIS structure for PPV prediction
32

33
34 **Fig. 10** PPV values obtained by proposed empirical equation versus the measured PPVs
35

36
37 **Fig. 11** R^2 values of measured and predicted PPV values for training and testing datasets using ANN
38

39
40 **Fig. 12** R^2 values of measured and predicted PPV values for training and testing datasets using ANFIS
41

42
43 **Fig. 13** Measured PPVs against predicted PPVs by Langefors - Kihlstrom (1963)
44

45
46 **Fig. 14** Measured PPVs against predicted PPVs by general predictor by Davies et al. (1964)
47

48
49 **Fig. 15** Measured PPVs against predicted PPVs by Bureau of Indian standard (1973)
50

51
52 **Fig. 16** Measured PPVs against predicted PPVs by Ghosh - Daemen predictor (1983)
53

54
55 **Fig. 17** Measured PPVs against predicted PPVs by CMRI by Roy (1993)
56
57
58
59
60
61

1
2
3
4
5
6
7
8
9
10
11
12
13
14
15
16
17
18
19
20
21
22
23
24
25
26
27
28
29
30
31
32
33
34
35
36
37
38
39
40
41
42
43
44
45
46
47
48
49
50
51
52
53
54
55
56
57
58
59
60
61
62
63
64
65

List of Tables:

Table 1 Recent works on PPV prediction using soft computation techniques

Table 2 Parameters used in the predictive model with their categories

Table 3 Recommended number of nodes for hidden layers [44]

Table 4 Performances of trained ANN models to predict PPV

Table 5 Performances of the 5 ANFIS models in predicting PPV

Table 6 Empirical PPV models

Table 7 Performance indices of all utilized models for prediction of PPV

Figure 1
[Click here to download high resolution image](#)

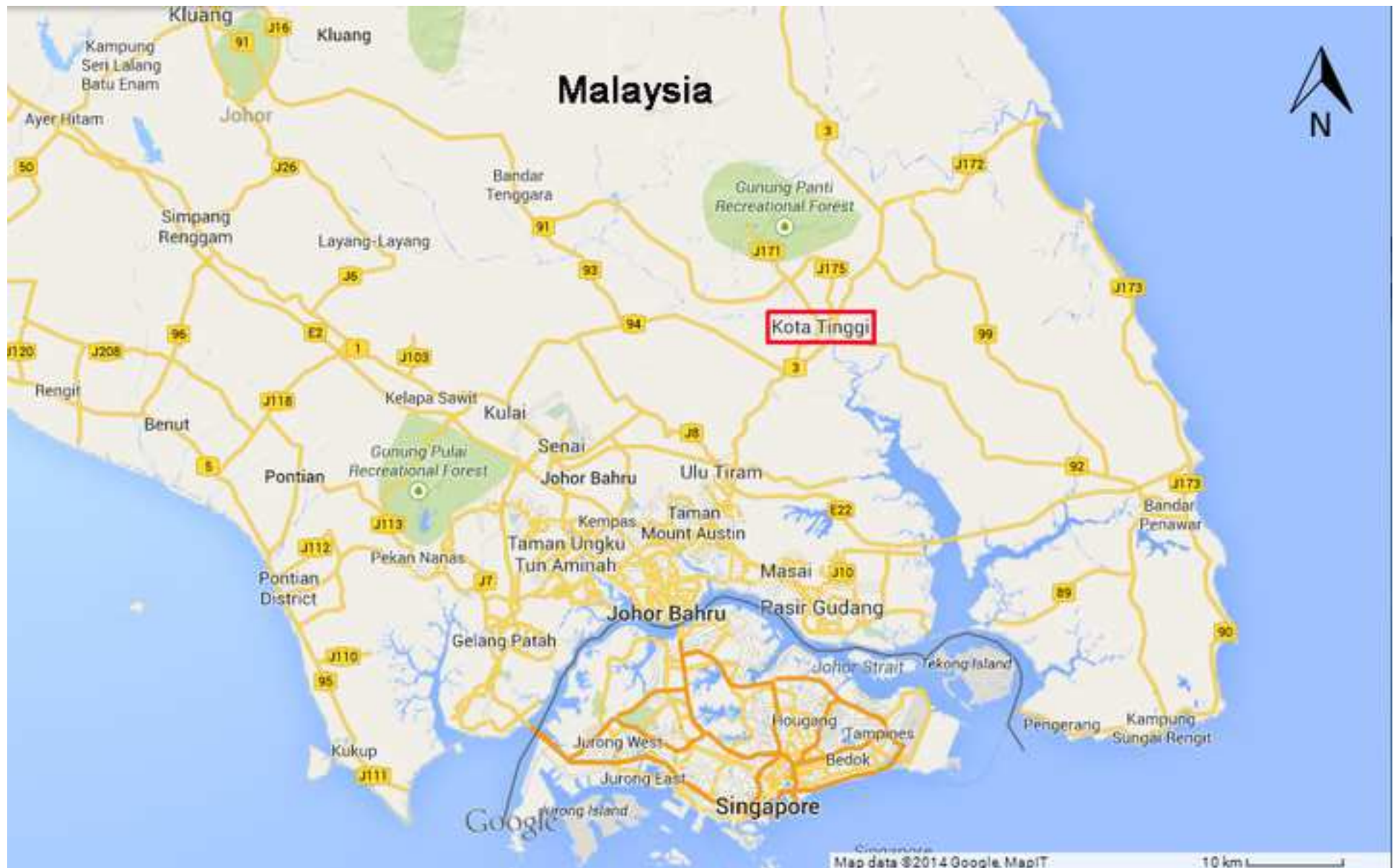


Figure 2
[Click here to download high resolution image](#)

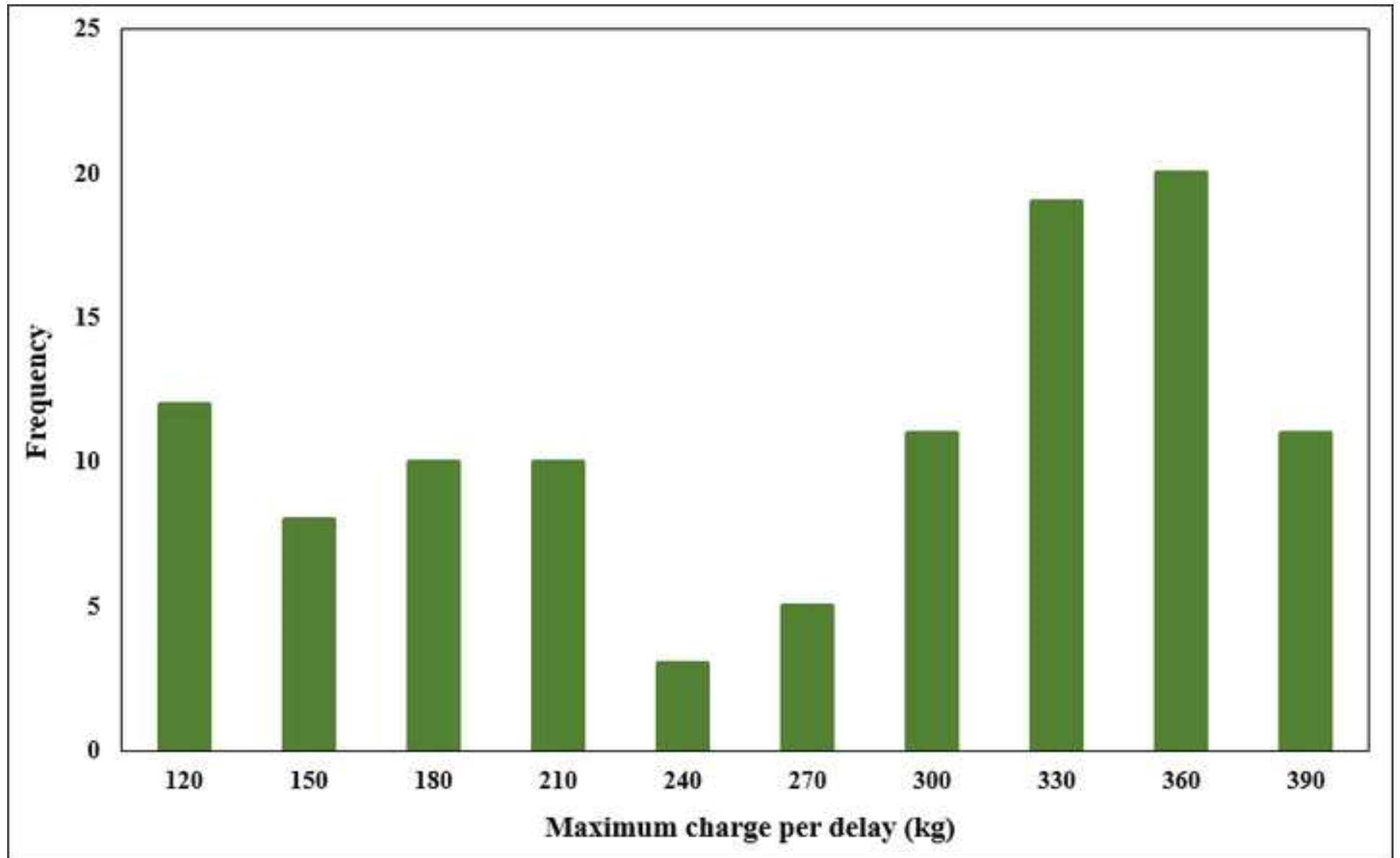


Figure 3
[Click here to download high resolution image](#)

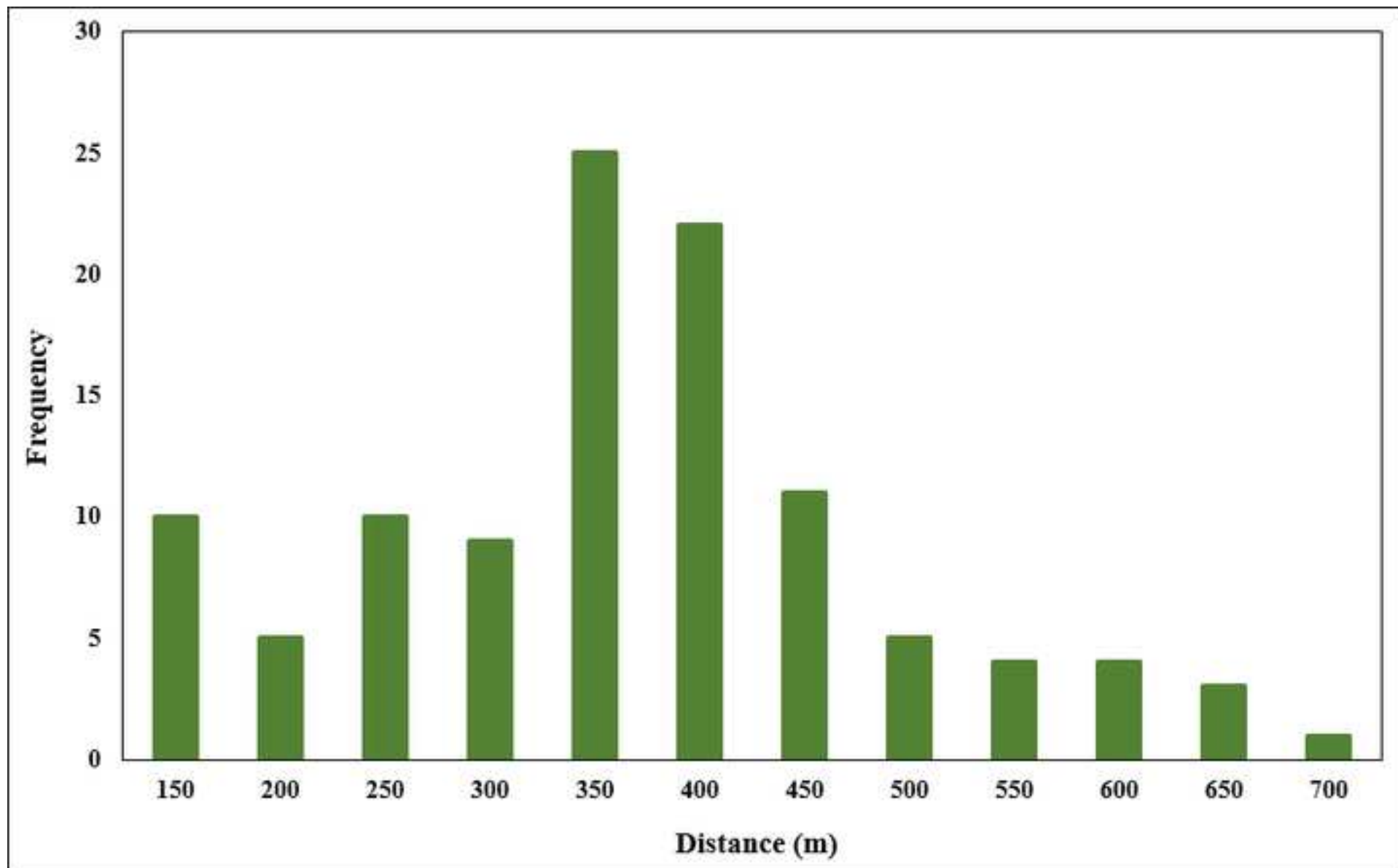


Figure 4
[Click here to download high resolution image](#)

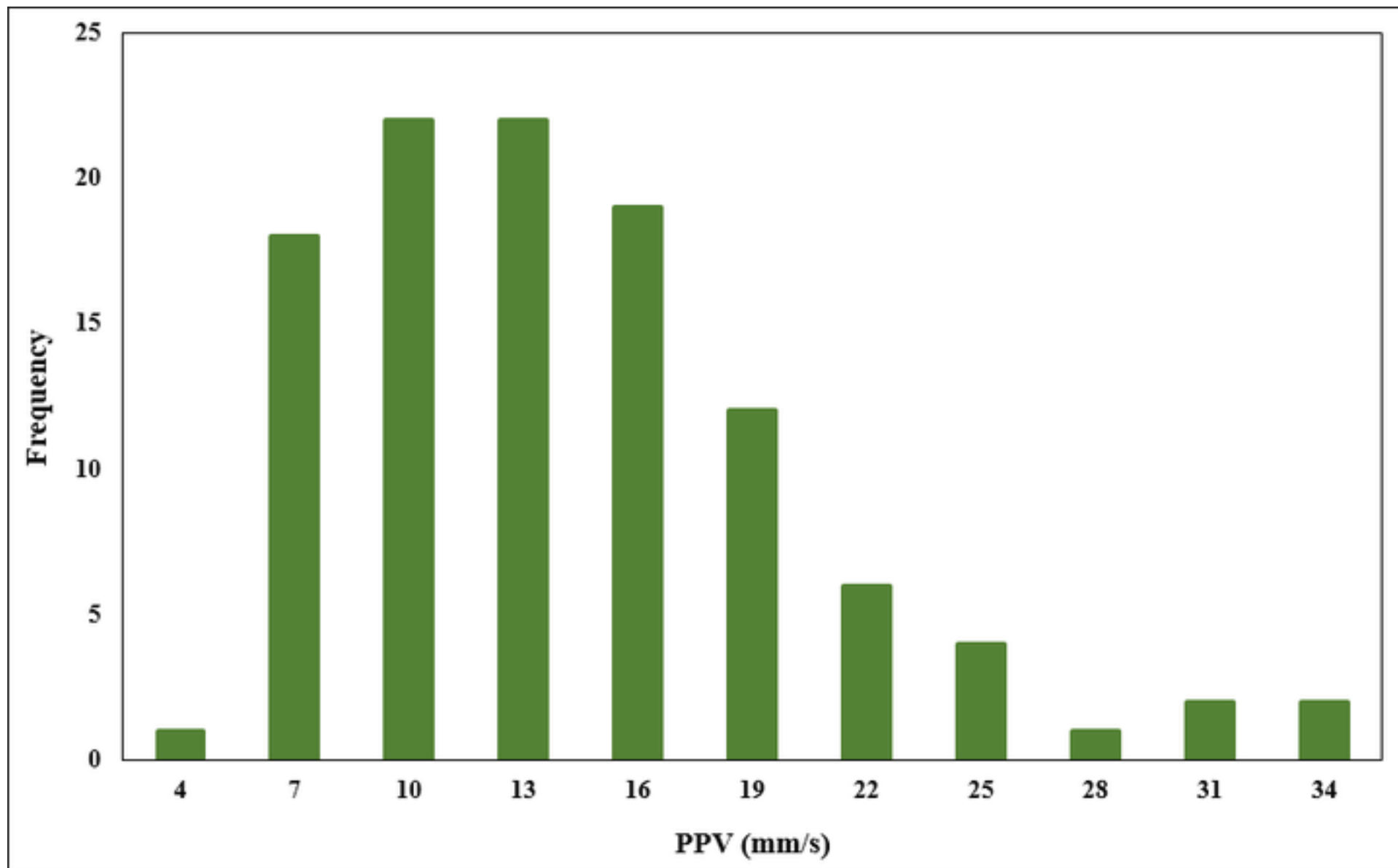


Figure 5
[Click here to download high resolution image](#)

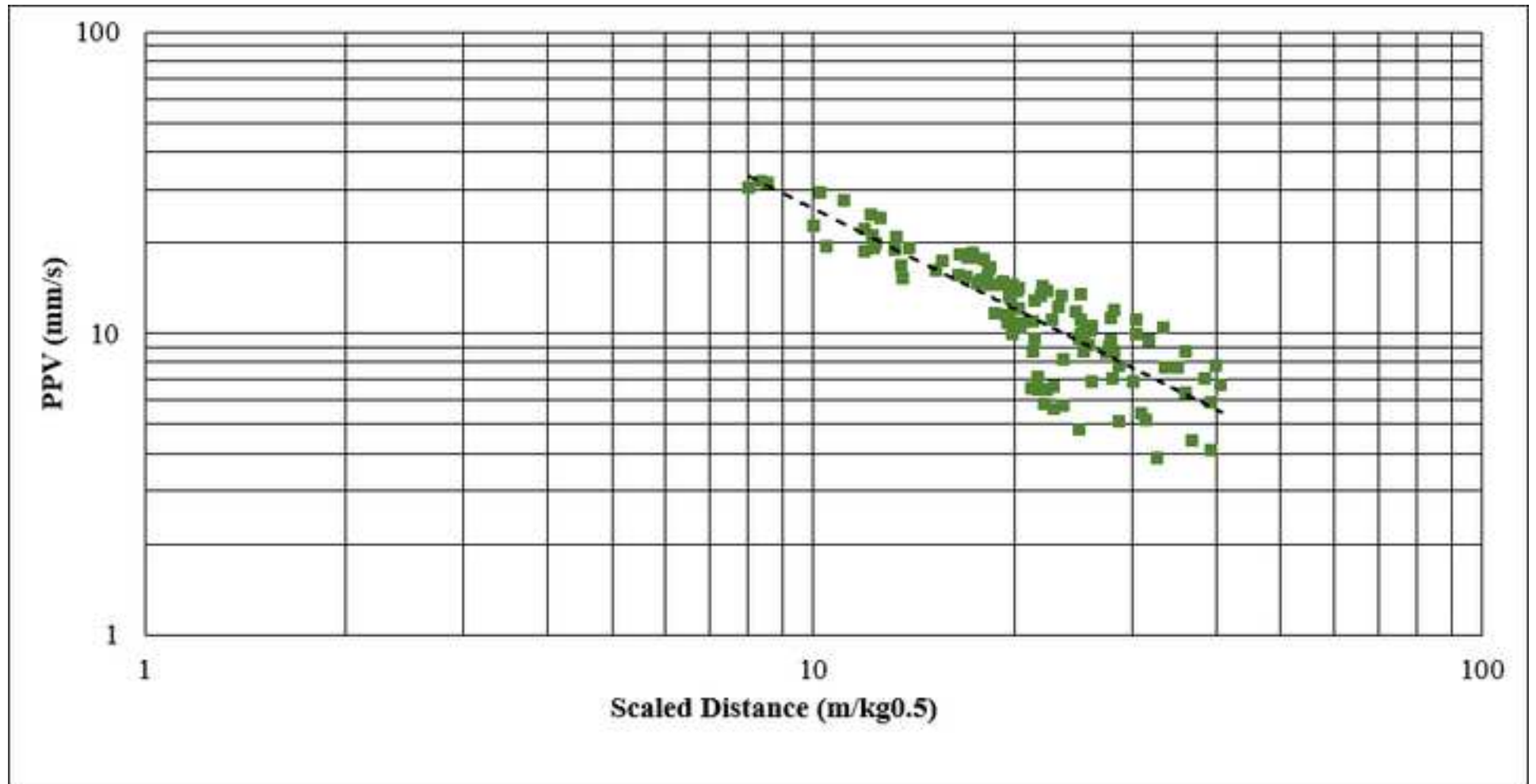


Figure 6
[Click here to download high resolution image](#)

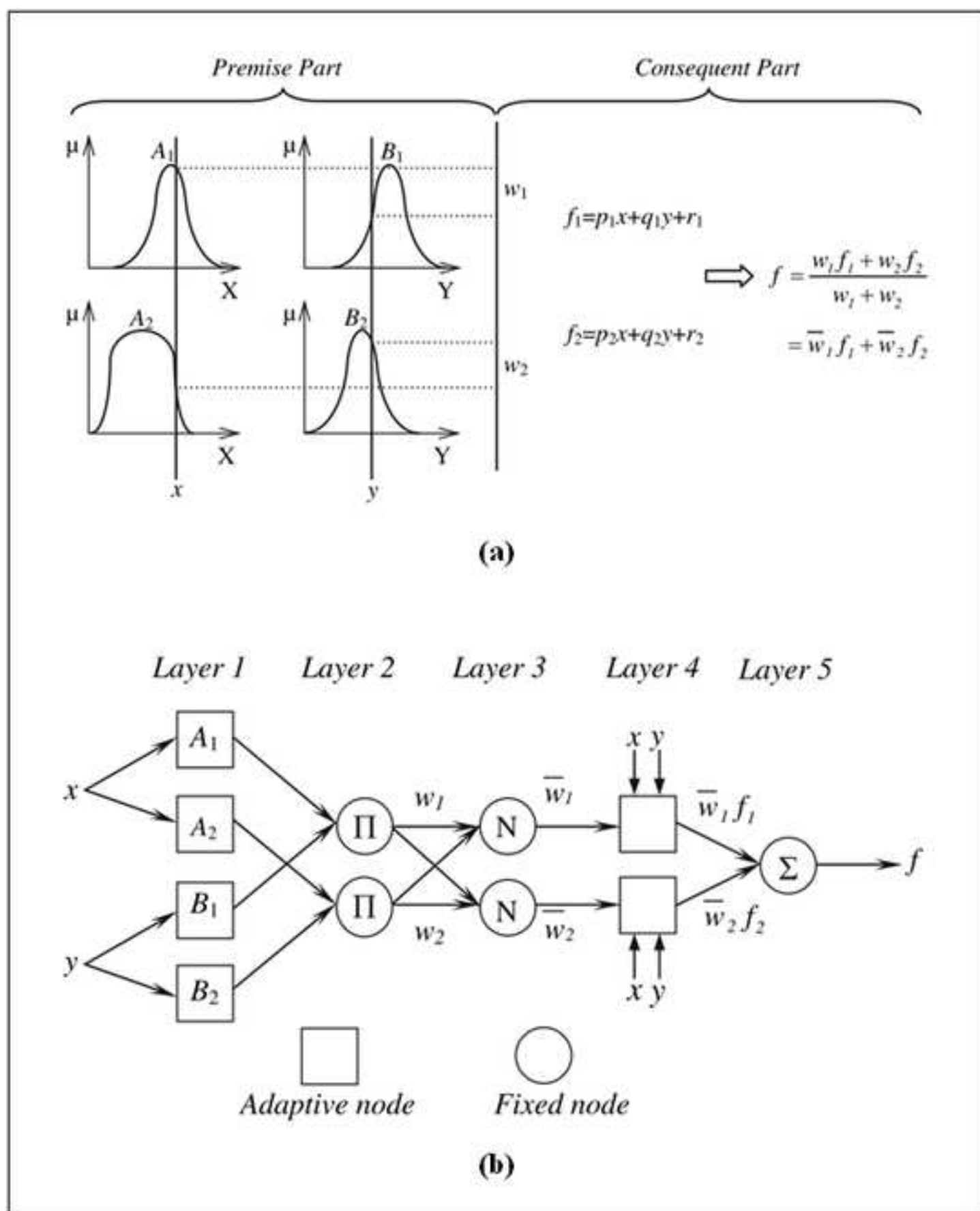


Figure 7
[Click here to download high resolution image](#)

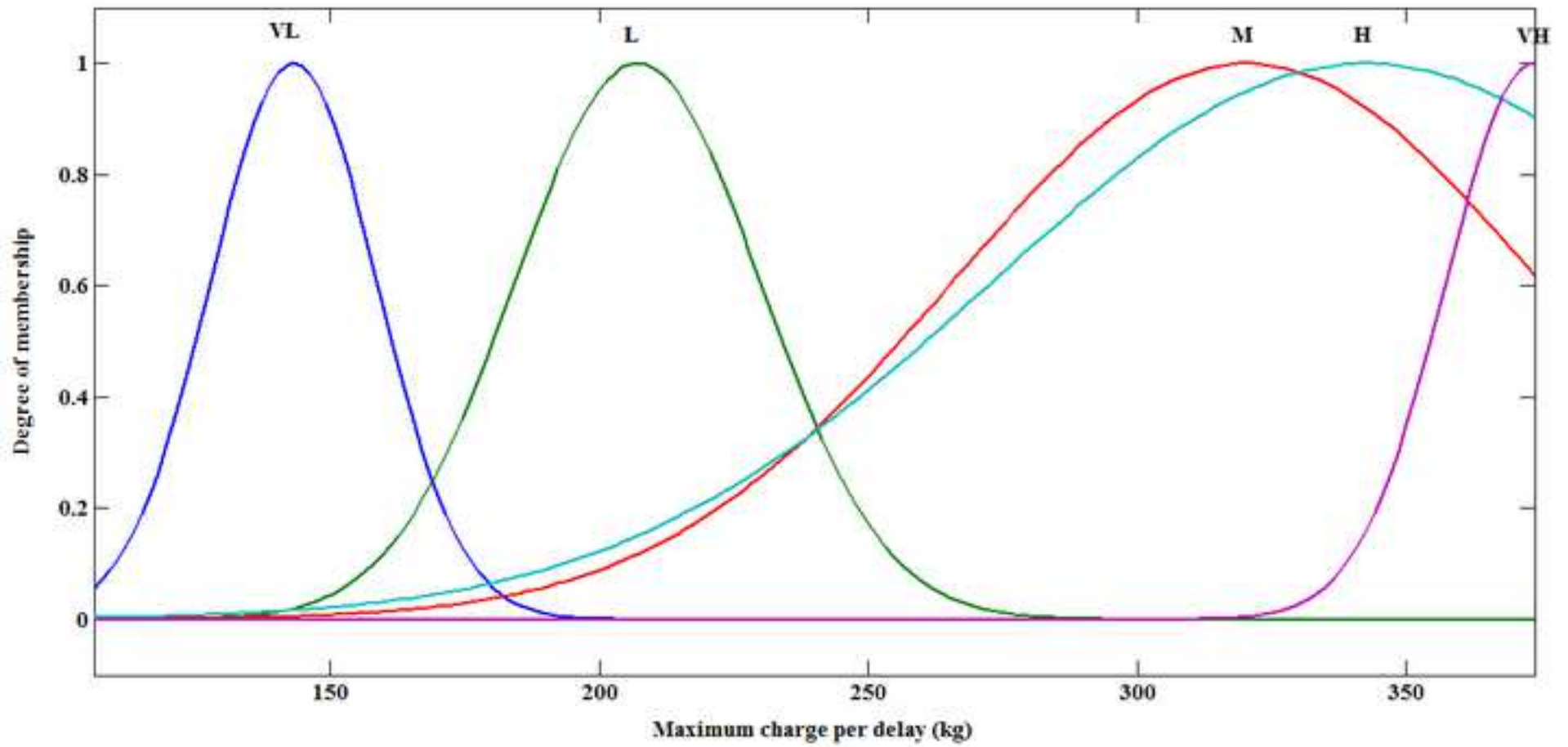


Figure 8
[Click here to download high resolution image](#)

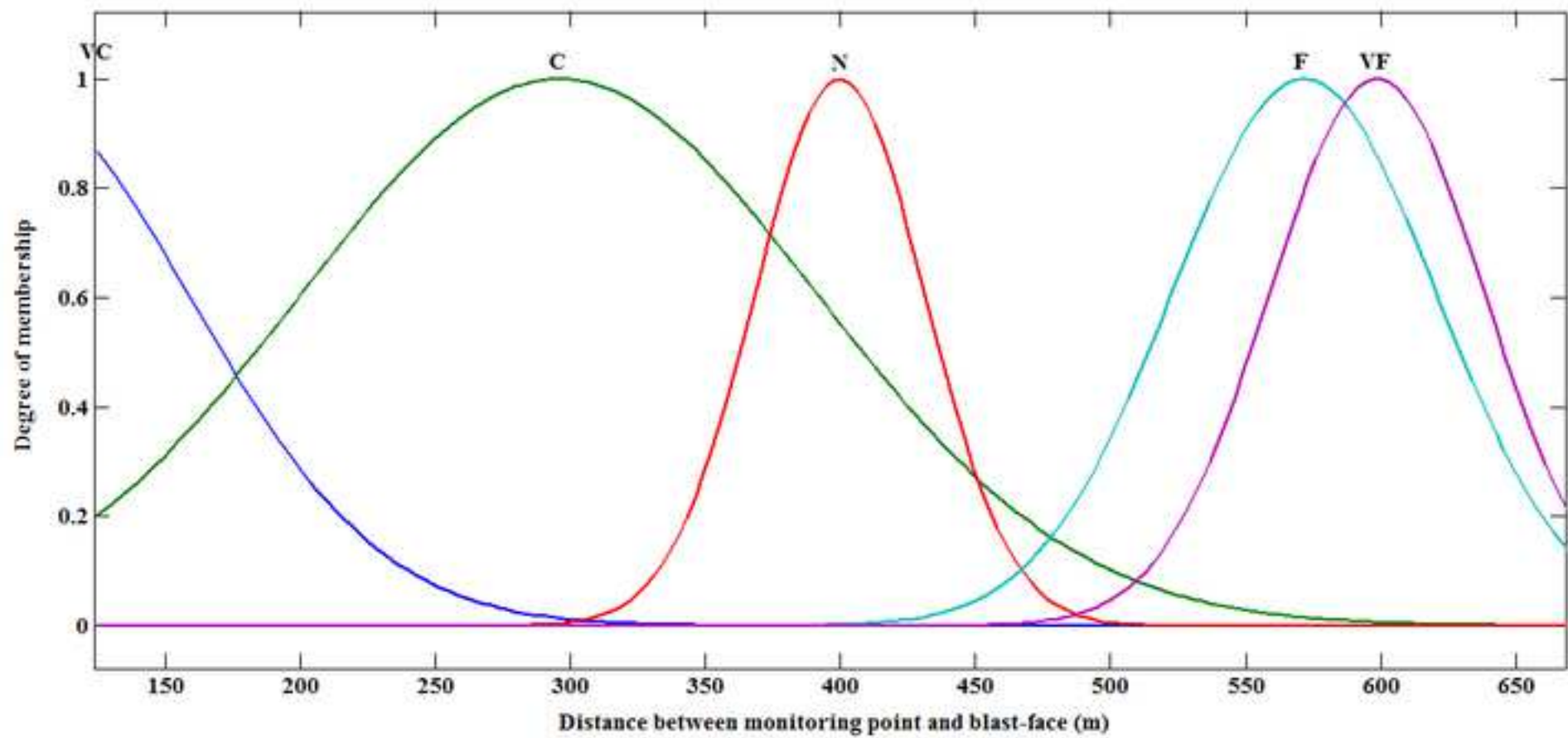


Figure 9
[Click here to download high resolution image](#)

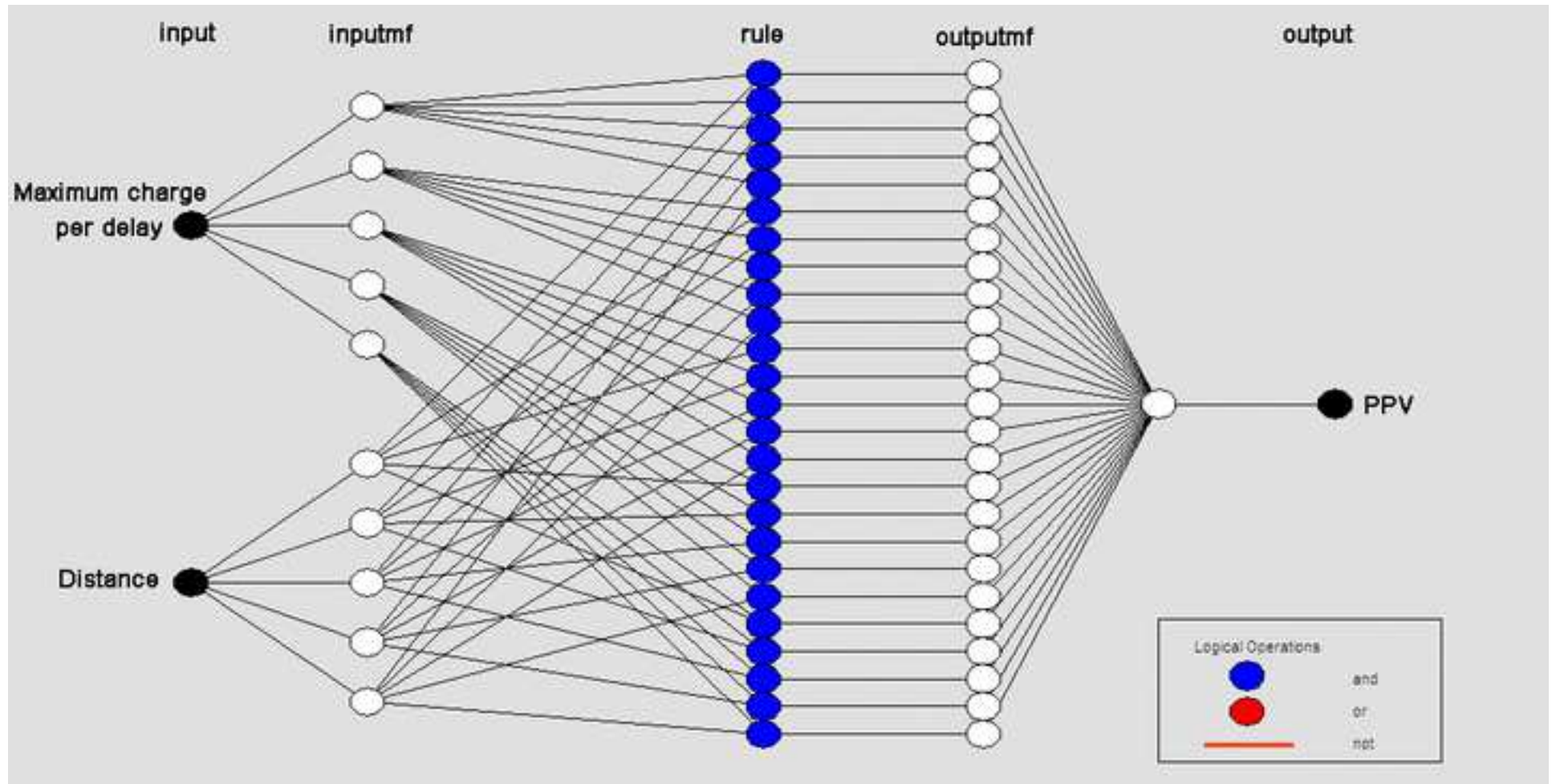


Figure 10
[Click here to download high resolution image](#)

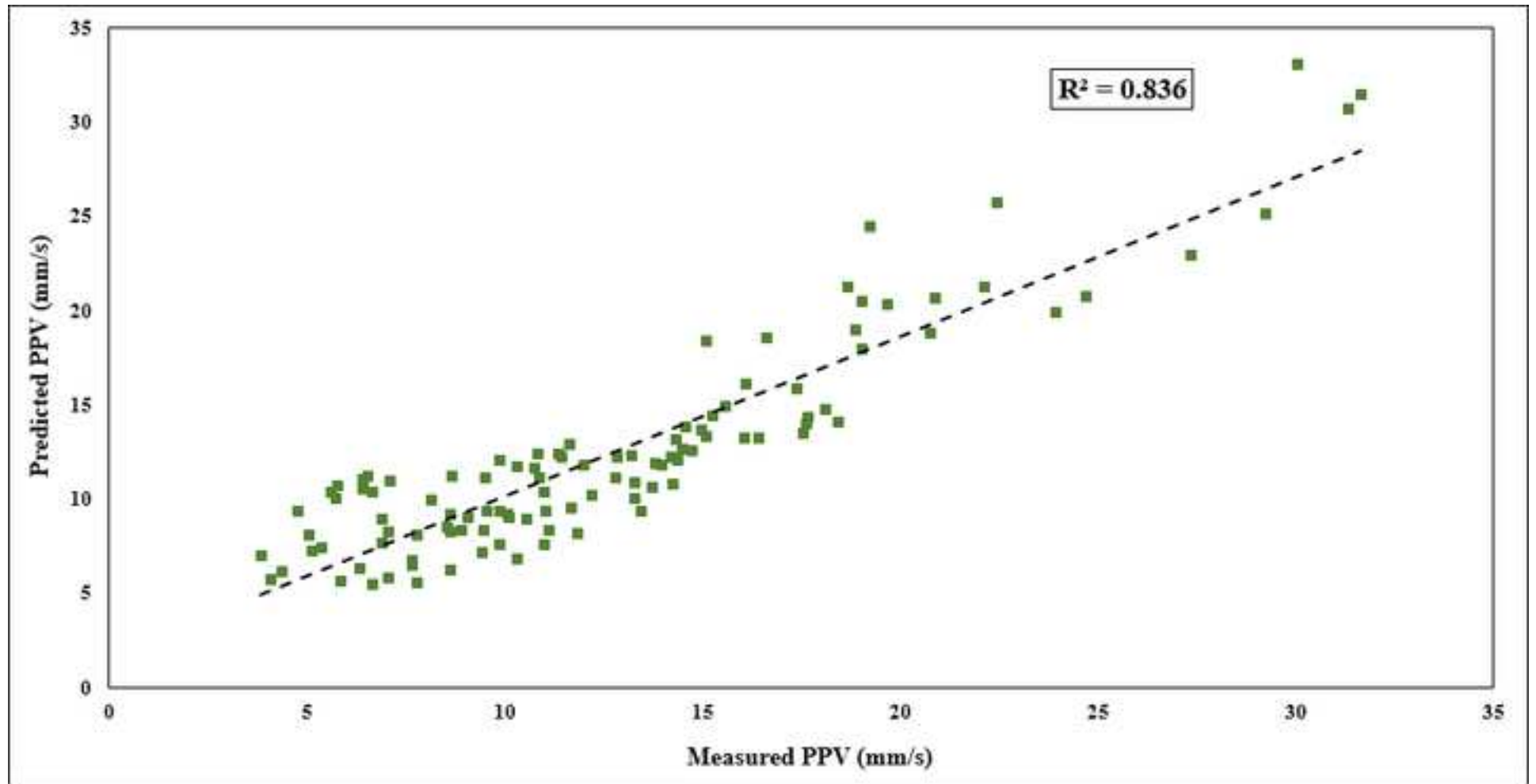


Figure 11
[Click here to download high resolution image](#)

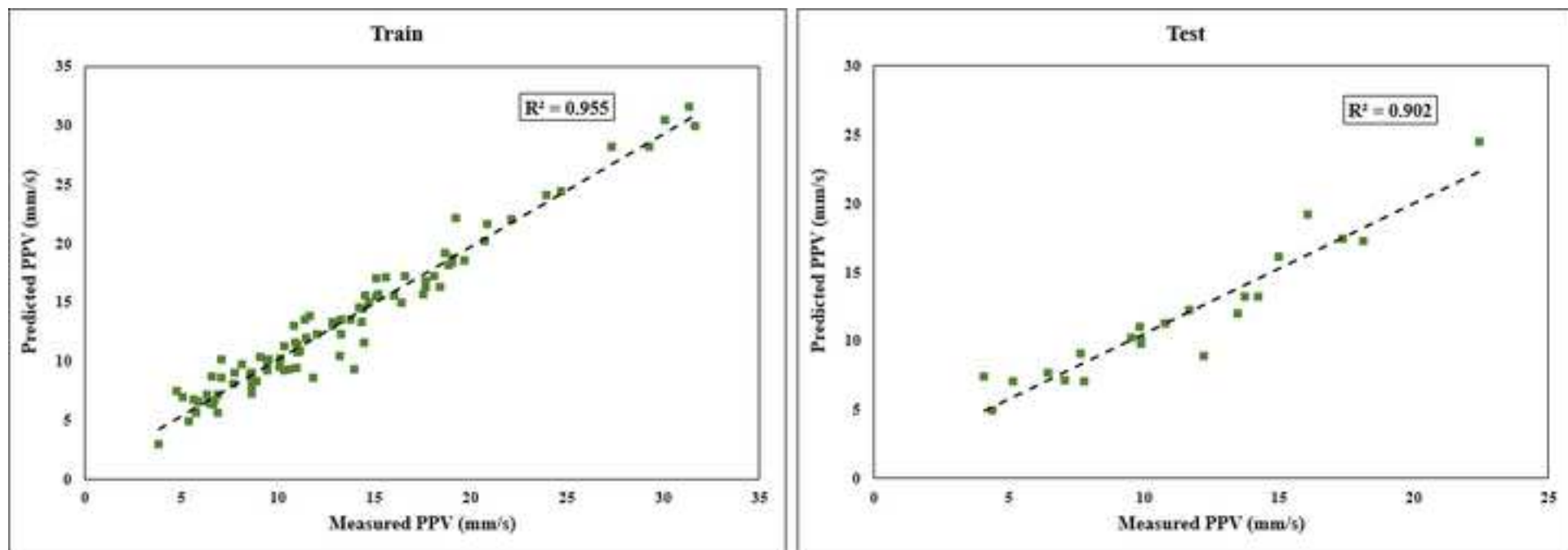


Figure 12
[Click here to download high resolution image](#)

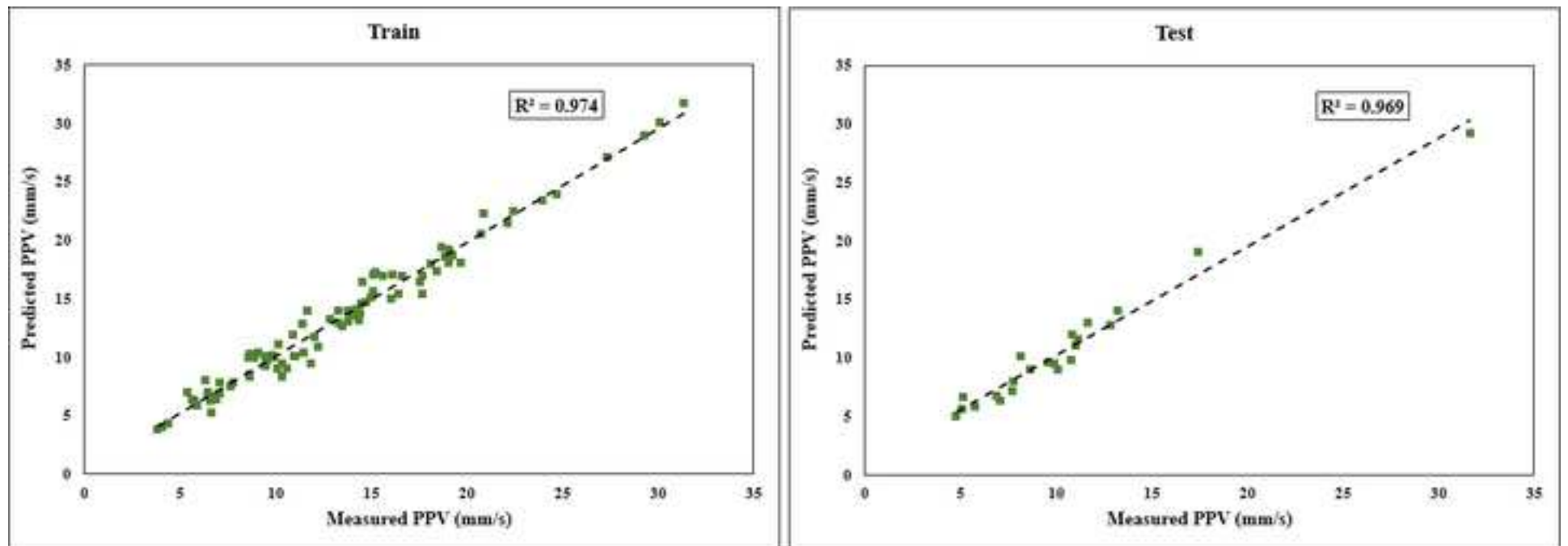


Figure 13
[Click here to download high resolution image](#)

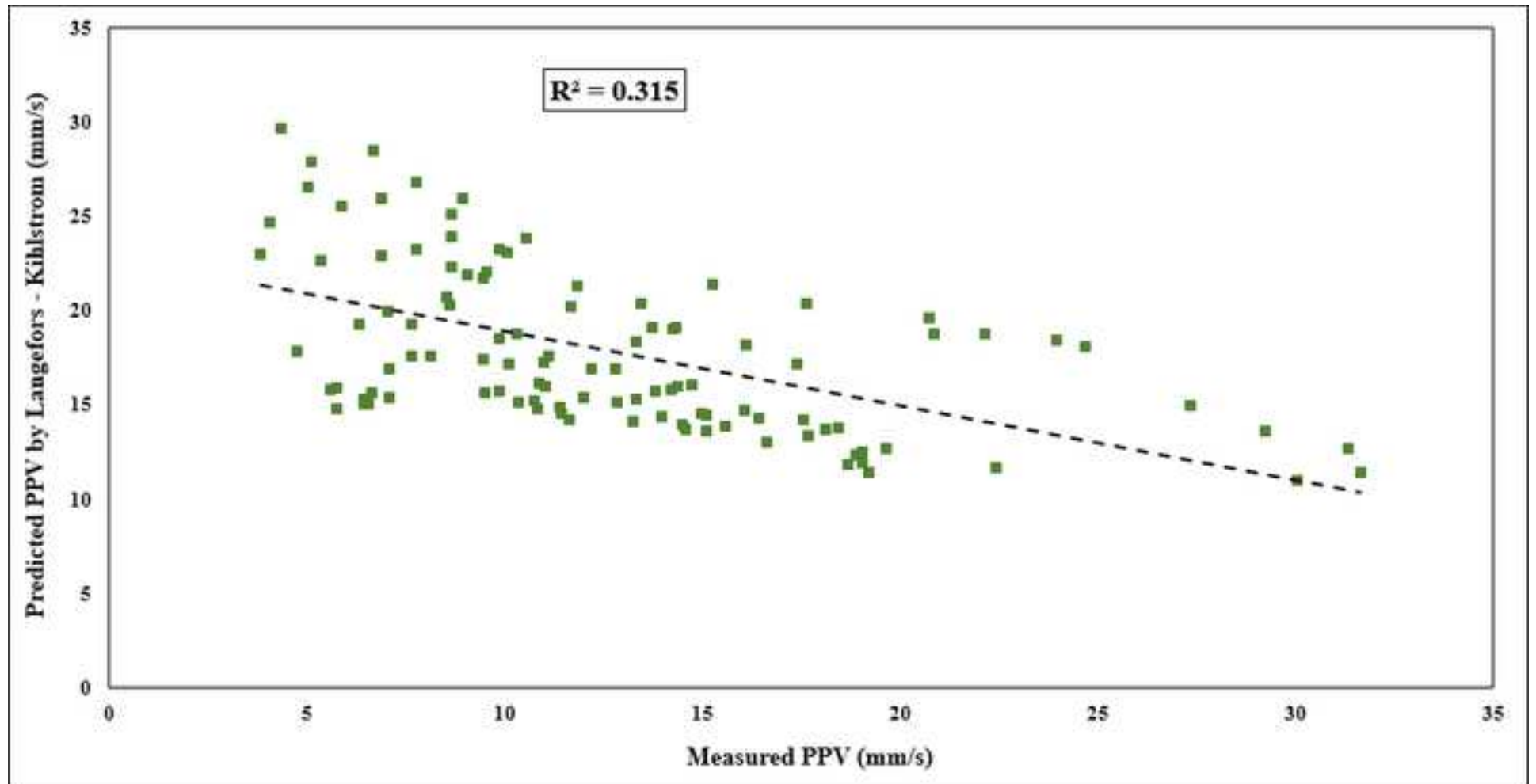


Figure 14
[Click here to download high resolution image](#)

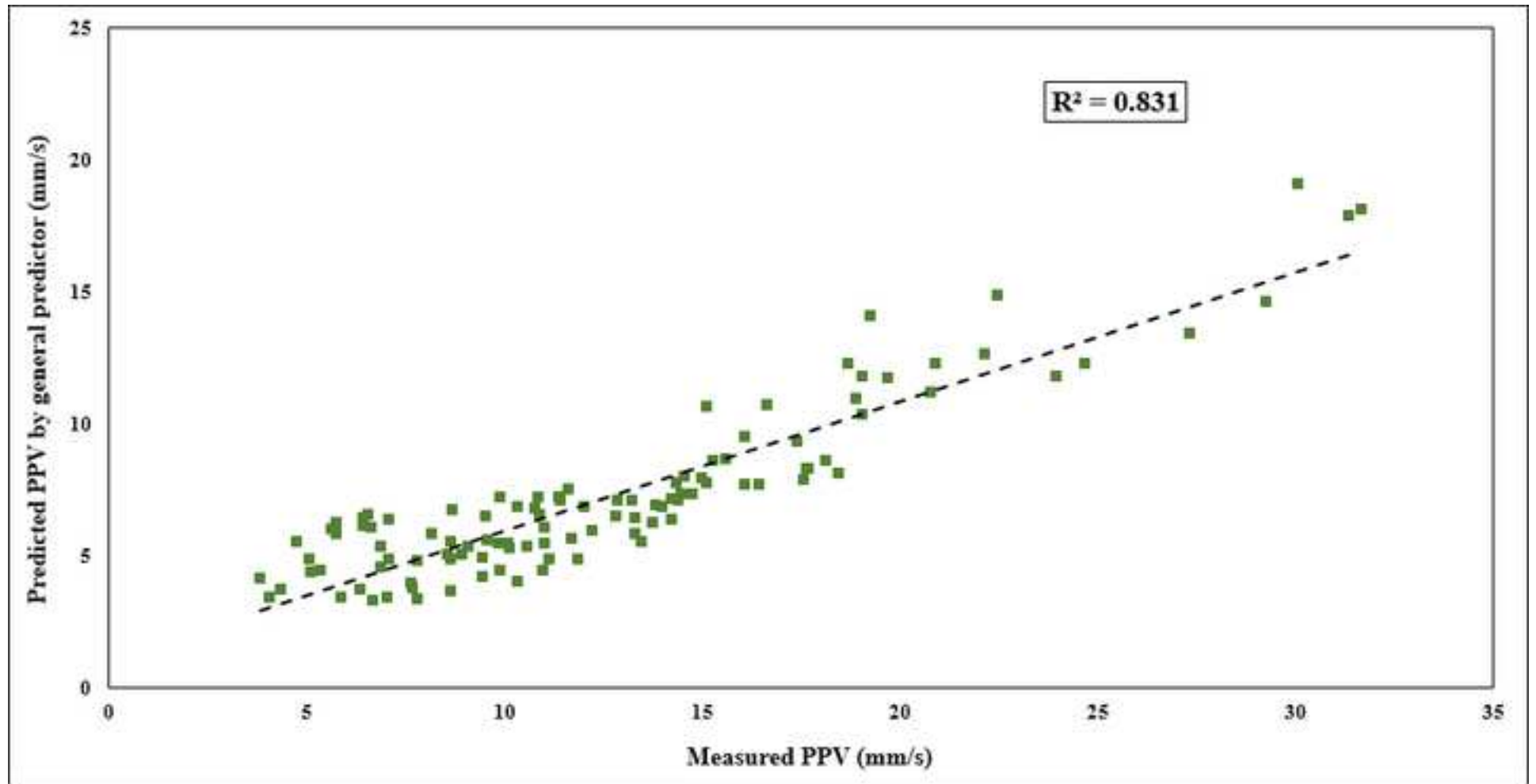


Figure 15
[Click here to download high resolution image](#)

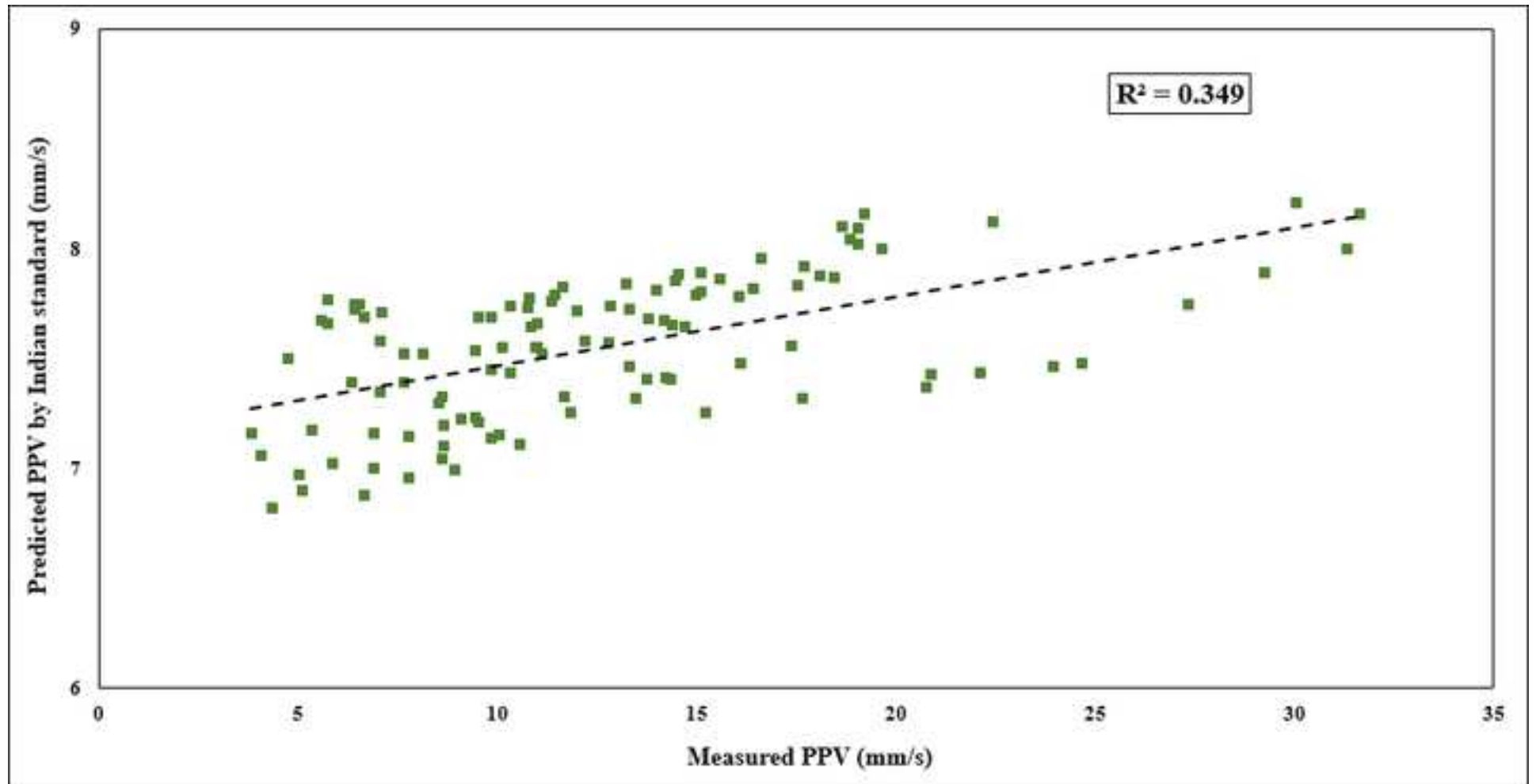


Figure 16
[Click here to download high resolution image](#)

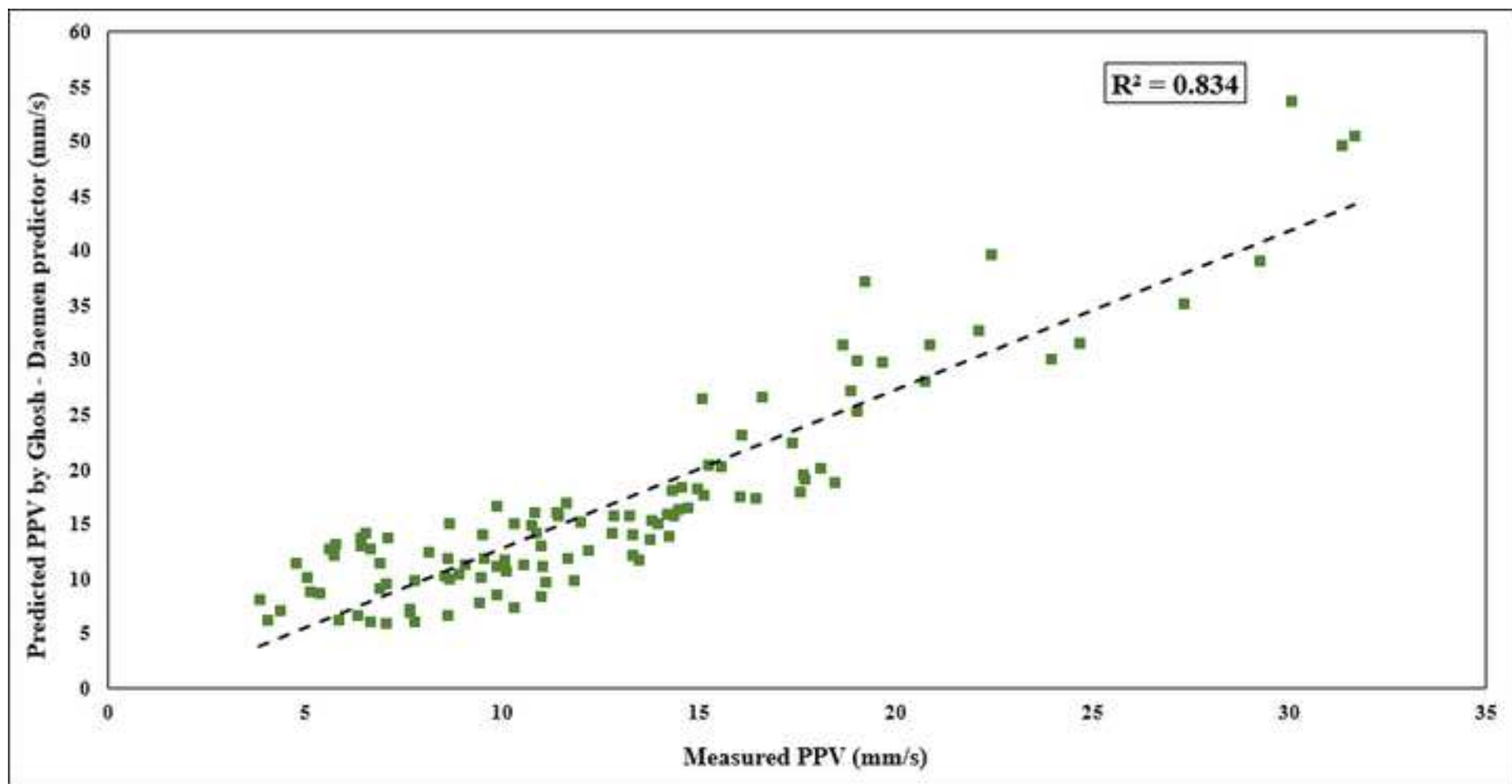


Figure 17
[Click here to download high resolution image](#)

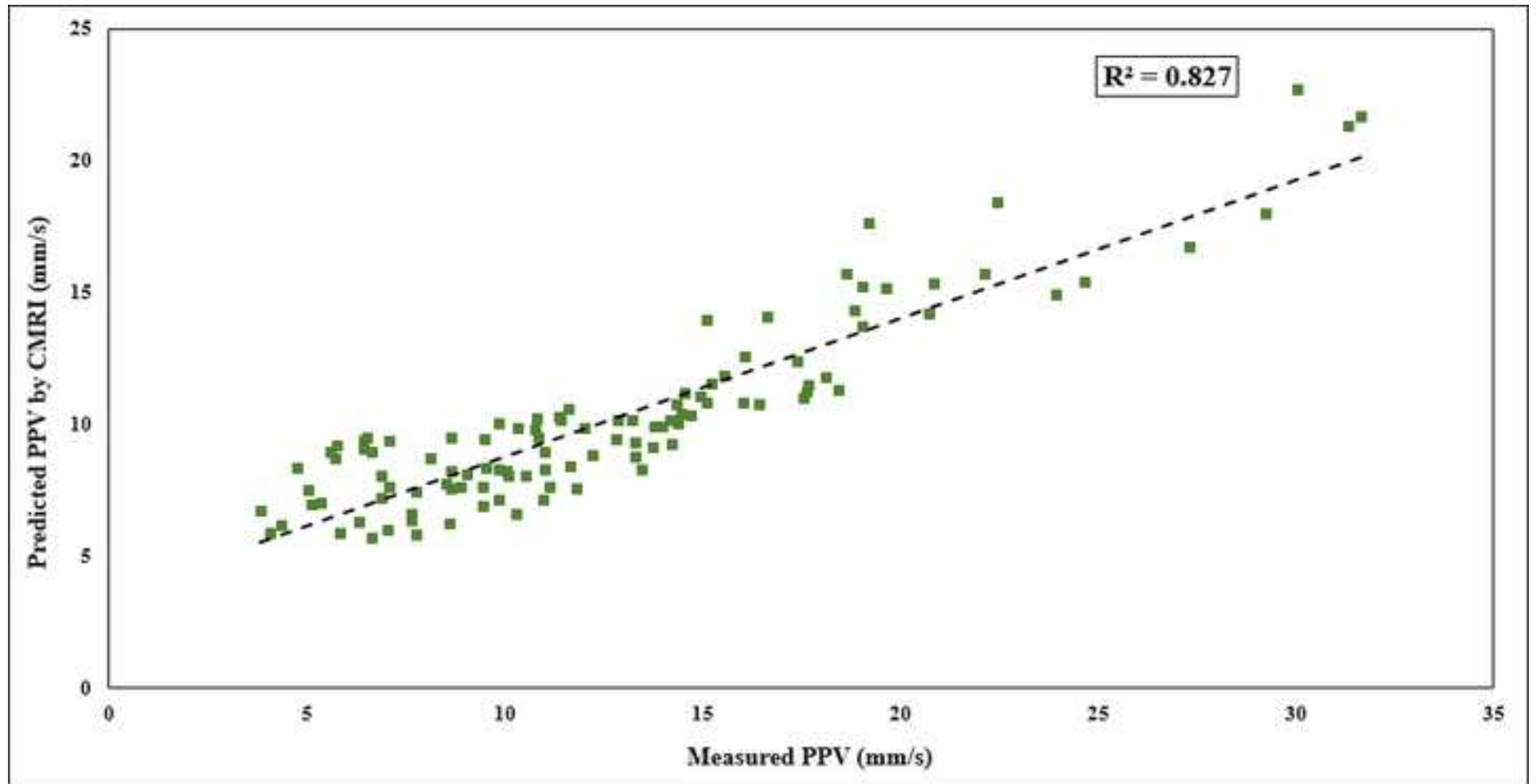


Table 1 Recent works on PPV prediction using soft computation techniques

Reference	Technique	Input	No. of dataset	R ²
Khandelwal and Singh (2009)	ANN	BI, S, B, HD, D, VOD, Vp, E, v, C	154	R ² = 0.98
Monjezi et al. (2010)	ANN	BS, N, D, UCS, C, DPR	269	R ² = 0.95
Monjezi et al. (2011)	ANN	HD, ST, D, C	182	R ² = 0.95
Khandelwal et al. (2011)	ANN	D, C	130	R ² = 0.92
Mohamed (2011)	ANN, FIS	D, C	162	R ² _{ANN} = 0.94 R ² _{FIS} = 0.90
Fisne et al. (2011)	FIS	D, C	33	R ² = 0.92
Li et al. (2012)	SVM	D, C	32	R ² = 0.89
Mohamadnejad et al. (2012)	SVM, ANN	D, C	37	R ² _{SVM} = 0.89 R ² _{ANN} = 0.85
Ghasemi et al. (2013)	FIS	B, S, ST, N, C, D	120	R ² = 0.95
Monjezi et al. (2013)	ANN	C, D, TC	20	R ² = 0.93
Jahed Armaghani et al. (2013)	ANN-PSO	HD, S, B, ST, PF, C, DI, N, RD, SD	44	R ² = 0.94
Hajihassani et al. (2014b)	ANN-ICA	BS, ST, D, C, Vp, E	95	R ² = 0.98
Ghoraba et al. (2015)	ANN	BS, D, C, ST, HD	115	R ² = 0.98

Spacing (S); burden (B); stemming (ST); powder factor (PF); specific drilling (SD); support vector machine (SVM); charge per delay (C); hole diameter (DI); hole depth (HD); rock density (RD); number of row (N); particle swarm optimization (PSO); sub-drilling (SD); distance from the blasting face (D); total charge (TC); blastability index (BI); velocity of detonation of explosive (VOD); p-wave (Vp); Young's modulus(E);poison's ratio(v); burden to spacing ration (BS); delay per rows (DPR); imperialist competitive algorithm (ICA).

Table 2 Parameters used in the predictive model with their categories

Parameter	Category	Unit	Symbol	Minimum	Maximum	Average
Maximum charge per delay	Input	(Kg)	MC	106	374	255.47
Distance*	Input	(m)	D	125	670	346.37
Peak particle velocity	Output	(mm/s)	PPV	3.83	31.65	12.72

* Distance between monitoring point and blast-face

Table 3 Recommended number of nodes for hidden layers (Sonmez et al. 2006)

Heuristic	Reference
$\leq 2 \times N_i + 1$	Hecht-Nielsen (1987)
$3N_i$	Hush (1989)
$(N_i + N_o)/2$	Ripley (1993)
$\frac{2 + N_o \times N_i + 0.5 N_o \times (N_o^2 + N_i) - 3}{N_i + N_o}$	Paola (1994)
$2N_i/3$	Wang (1994)
$\sqrt{N_i \times N_o}$	Masters (1994)
$2N_i$	Kaastra and Boyd (1996)
	Kannellopoulos and Wilkinson (1997)

N_i : number of input neuron, N_o : number of output neuron.

Table 4 Performances of trained ANN models to predict PPV

Model No.	Nodes in hidden layers	Network Result									
		Iteration 1		Iteration 2		Iteration 3		Iteration 4		Iteration 5	
		RMSE		RMSE		RMSE		RMSE		RMSE	
		Train	Test	Train	Test	Train	Test	Train	Test	Train	Test
1	1	2.709	2.778	2.755	2.387	2.608	3.013	2.655	2.839	2.714	2.587
2	2	2.585	2.583	2.689	2.705	2.071	2.781	2.206	2.759	2.329	2.182
3	3	1.865	2.507	2.112	2.539	2.091	2.438	1.976	2.665	2.059	2.410
4	4	1.949	2.220	2.021	2.118	2.163	2.471	2.055	2.393	1.825	2.491
5	5	1.425	1.777	1.684	2.285	1.662	2.250	1.377	2.173	1.418	1.673
6	6	1.261	1.726	1.327	1.538	1.576	1.653	1.597	1.654	1.698	2.473

Table 5 Performances of the 5 ANFIS models in predicting PPV

ANFIS Model	RMSE	
	Train	Test
1	1.114	1.642
2	1.217	1.599
3	1.020	1.252
4	0.983	1.017
5	1.303	1.595

Table 6 Empirical PPV models

Reference	Equation	Site Constant for Granite
Langefors - Kihlstrom (1963)	$PPV = K[\sqrt{(MC/D^{2/3})}]^B$	K: 44.43, B: -1.18
General predictor by Davies et al. (1964)	$PPV = KD^{-B}(MC)^A$	K: 212.27, B: 1.09, A: 0.52
Bureau of Indian Standard (1973)	$PPV = K[(MC/D^{2/3})]^B$	K: 6.33, B: 0.22
Ghosh - Daemen predictor (1983)	$PPV = K[D/\sqrt{MC}]^{-B}e^{-\alpha D}$	K: 780.36, B: 1.26, α : 0.0004
CMRI by Roy (1993)	$PPV = n + K[D/\sqrt{MC}]^{-1}$	K: 168.91, n: 1.57

PPV: Peak particle velocity (mm/s), *MC*: Maximum charge per delay (kg), *D*: Distance between blast face and vibration monitoring point (m), *K*, *B*, *A*, α , *n*: Site constants.

Table 7 Performance indices of all utilized models for prediction of PPV

Predictive Model	Performance Indices		
	R²	RMSE	VAF (%)
Langefors - Kihlstrom	0.315	10.473	-128.274
General predictor	0.831	6.391	69.293
Indian Standard	0.349	7.821	6.024
Ghosh - Daemen predictor	0.834	6.233	37.996
CMRI	0.827	4.078	72.068
Proposed model based on USBM	0.836	2.469	83.629
ANN	0.949	1.372	94.895
ANFIS	0.973	0.987	97.345